

Perspective on Kinematic Modeling

VICES Sept. 28–Oct. 2, 2014

Ralph Archuleta
Department of Earth Science
University of California, Santa Barbara



Earthquake Source Models

- ① **Point Source {Maruyama, 1963; Burridge and Knopoff, 1964}**
- ② **Finite Fault--Kinematic {Haskell, 1964}**
- ③ **Finite Fault--Dynamic {Kostrov, 1964}**

Maruyama 1963

BULLETIN OF THE EARTHQUAKE
RESEARCH INSTITUTE
Vol. 41 (1963), pp. 407-436

31. On the Force Equivalents of Dynamical Elastic Dislocations with Reference to the Earthquake Mechanism.*

By TAKUO MARUYAMA,

Graduate School, University of Tokyo.
(Read April 23, 1963.—Received June 29, 1963.)

Introduction.

Methods of determining the nature of the motion at the foci of earthquakes have been developed by many seismologists (Hodgson 1959, 1961; Honda 1962). In every method one is led to correlate seismic observations with mathematical solutions to certain problems in elasticity theory. Recently the mathematical models on which these solutions are based have been examined from the viewpoint of dislocation theory.

A. V. Vvedenskaya (1956) found a system of forces which may be equivalent to a rupture accompanied by slipping in the theory of dislocations (Nabarro 1951). She has developed her method on the consideration that a rupture accompanied by slipping is the most probable form of movement in the earthquake foci under the conditions which occur in the earth's crust and in the upper part of the mantle, in which stresses may be supposed to have a considerable duration. It was interesting that the source in this case can be constructed by integration of the well-known force system type II, i. e. a pair of coplanar couples with moments of equal magnitude acting at right angles to one another, along the fault surface. However, Nabarro's formulae on which this method is based were obtained by replacing the system of static forces which is found in a static dislocation by the system of dynamic forces which has step function time dependence. A. V. Vvedenskaya (1959), after F. R. N. Nabarro, obtained formulae for the case of sudden formation of general Volterra dislocations (Volterra 1907), but she did not treat of the basis of the theory of general dynamic dislocations.

J. A. Steketee (1958 a, b) suggested independently that the theory of dislocations might be the proper tool for problems connected with faultplane studies of earthquakes and with fracture zones in the

* Communicated by S. MIYAMURA.

Burridge and Knopoff 1964

Bulletin of the Seismological Society of America. Vol. 54, No. 6, pp. 1875-1888. December, 1964

BODY FORCE EQUIVALENTS FOR SEISMIC DISLOCATIONS

By R. BURRIDGE AND L. KNOPOFF

ABSTRACT

An explicit expression is derived for the body force to be applied in the absence of a dislocation, which produces radiation identical to that of the dislocation. This equivalent force depends only upon the source and the elastic properties of the medium in the immediate vicinity of the source and not upon the proximity of any reflecting surfaces. The theory is developed for dislocations in an anisotropic inhomogeneous medium; in the examples isotropy is assumed. For displacement dislocation faults, the double couple is an exact equivalent body force.

1. INTRODUCTION

The interest in the "force equivalent" problem antedates its solution by a considerable number of years. The debates over "single couple" and "double couple" earthquake focal mechanisms have by now been well viewed and reviewed. For a discussion of the problem of earthquake source mechanisms see Stauder (1962).

It has been pointed out by several authors (Knopoff and Gilbert, 1960; Balakina, Shirokova, and Vvedenskaya, 1960) that the solution to the problem of the seismic radiation from a suddenly occurring earthquake in the earth's interior is likely to be connected with the solution to a "dislocation" problem, or, in the terminology of Baker and Copson (1950), to a "saltus" problem. In these problems the displacement field or stress field undergoes the more or less sudden creation of a discontinuity across the "fault" surface.

Perhaps the most complete solution to the dislocation problem has been given by Knopoff and Gilbert. These authors showed that a model of an earthquake can be represented as a linear combination of the solutions to a number of fundamental problems. The remaining problem, that of determining the appropriate linear combinations, was not attempted.

Although Knopoff and Gilbert were primarily interested in the radiation patterns from their various dislocation models they also provided the force equivalents that would produce the same first motions as each of their sources. In this paper we find the force equivalents for physically and mathematically reasonable dislocation models.

Nabarro (1951) obtained the radiation from a spreading dislocation by essentially the same method as Knopoff and Gilbert but in a less explicit form. He had in mind mainly metallurgical applications. Recently Maruyama (1963) has attempted to derive the force equivalents but his results are obscured by algebraic detail associated with the explicit expression of a certain Green's function.

In this paper we specifically exclude consideration of the radiation pattern. We are concerned with the body force which would have to be applied in the absence of the fault to produce the same radiation (in all respects, not only first motions) as a given dislocation. We find that the force equivalent depends only upon the source mechanism and the elastic properties of the medium in the immediate vicinity of the fault and not upon any reflecting surfaces or other inhomogeneities which may be present in the medium. The theory is developed for dislocations in

TOTAL ENERGY AND ENERGY SPECTRAL DENSITY OF ELASTIC WAVE RADIATION FROM PROPAGATING FAULTS

By N. A. HASKELL

ABSTRACT

Starting with a Green's function representation of the solution of the elastic field equations for the case of a prescribed displacement discontinuity on a fault surface, it is shown that a shear fault (relative displacement parallel to the fault plane) is rigorously equivalent to a distribution of double-couple point sources over the fault plane. In the case of a tensile fault (relative displacement normal to the fault plane) the equivalent point source distribution is composed of force dipoles normal to the fault plane with a superimposed purely compressional component. Assuming that the fault break propagates in one direction along the long axis of the fault plane and that the relative displacement at a given point has the form of a ramp time function of finite duration, T , the total radiated P and S wave energies and the total energy spectral densities are evaluated in closed form in terms of the fault plane dimensions, final fault displacement, the time constant T , and the fault propagation velocity. Using fault parameters derived principally from the work of Ben-Menahem and Toksoz on the Kamehatka earthquake of November 4, 1952, the calculated total energy appears to be somewhat low and the calculated energy spectrum appears to be deficient at short periods. It is suggested that these discrepancies are due to over-simplification of the assumed model, and that they may be corrected by (1) assuming a somewhat roughened ramp for the fault displacement time function to correspond to a stick-slip type of motion, and (2) assuming that the short period components of the fault displacement wave are coherent only over distances considerably smaller than the total fault length.

INTRODUCTION

Knopoff and Gilbert (1960) have used a Green's function integral representation of the solution of the elastic wave equations in an infinite medium to discuss the radiation pattern of first motions from a moving fault. In the present paper we shall employ the same approach to calculate the total radiation from a moving fault of finite length.

In the compact tensor notation of de Hoop (1958) the elastic displacements, $u_i(x_1, x_2, x_3, t)$, in a volume, V , bounded by a surface, S , are given by

$$u_i(x_1, x_2, x_3, t) = \iiint_V G_{ij} f_j dV + \iint_S c_{ijk} G_{ij} \partial u_k / \partial \xi_1 | n_1 ds + (\partial / \partial x_1) \iint_S c_{ijk} G_{ij} [u_k] n_1 ds \quad (1)$$

where

- x_1, x_2, x_3 = Cartesian coordinates of point at which u_i is to be evaluated
- ξ_1, ξ_2, ξ_3 = Cartesian coordinates of the point of integration in V and on S .
- f_j = body force per unit volume
- $c_{ijk} = \rho(\alpha^2 - 2\beta^2)\delta_{ij}\delta_{ik} + \rho\beta^2(\delta_{ij}\delta_{ik} + \delta_{ij}\delta_{kl})$

Haskell 1964

Let the (x_1, x_2) plane be the fault plane, with the positive x_2 axis normal to the fault plane on the S^+ side, and let the positive x_1 axis be parallel to the common direction of fault displacement and propagation. Then $n_1^+ = -\delta_{11}$ and $D_1 = \delta_{11}D$. In this case equation (9) becomes

$$4\pi r \dot{u}_i(\mathbf{x}, t) = 2(\beta/\alpha)^2 \iint_{S^+} (\alpha r)^{-1} \gamma_1 \gamma_1 \gamma_1 \dot{D}(\xi, t - r/\alpha) ds + \iint_{S^+} (\beta r)^{-1} [-2\gamma_1 \gamma_1 \gamma_1 + \gamma_1 \delta_{11} + \gamma_1 \delta_{33}] \dot{D}(\xi, t - r/\beta) ds \quad (10)$$

The integrands in equation (10) are exactly the same as those that one would obtain by considering the fault plane to be covered with a distribution of double couple sources, the common moment of the component couples having an areal density $M(\xi, t) = \rho\beta^2 D(\xi, t)$.

In accordance with the definition of radiated energy previously given, we may consider the point of observation, \mathbf{x} to be sufficiently remote that the radial distance, r , and the direction cosines, γ_i , are constant over the area of the fault to any desired degree of approximation. We further assume that the fault plane is rectangular with length L in the direction of propagation and width w in the transverse direction. We also suppose that the dependence of D on the transverse coordinate does not vary with time. Equation (10) may then be written as

$$4\pi r \dot{u}_i(\mathbf{x}, t) = 2(\beta/\alpha)^2 \gamma_1 \gamma_1 \gamma_1 w I_a + (-2\gamma_1 \gamma_1 \gamma_1 + \gamma_1 \delta_{11} + \gamma_1 \delta_{33}) w I_b \quad (11)$$

where

$$I_a = \int_0^L \dot{D}(\xi, t - r/\alpha) d\xi$$

$$I_b = \int_0^L \dot{D}(\xi, t - r/\beta) d\xi \quad (12)$$

\dot{D} is the displacement averaged over the width of the fault and $\xi = \xi_1$. Introducing a

Kostrov 1964

SELSIMILAR PROBLEMS OF PROPAGATION OF SHEAR CRACKS

(AVTOMODEL'NYE ZADACHI O RASPROSTRANENII
TRESHCHIN KASATEL'NOGO RAZRYVA)

PMM Vol.28, № 5, 1964, pp. 889-898

B.V. KOSTROV
(Moscow)

(Received April 10, 1964)

Two- and three-dimensional problems of nonsteady propagation of cracks are considered in a medium subjected to a homogeneous shear. The two-dimensional problem is completely analogous to Broberg's problem [1] of a tension crack, but is solved by a considerably simpler method. The joint investigation of the two- and three-dimensional cases also has the advantage that a number of intermediate results of the two-dimensional problem form the basis for the solution of the three-dimensional case.

The axisymmetric problem of propagation of a tension crack, the three-dimensional analogue of Broberg's problem, was solved in paper [2]. In contrast to the problem, the one which is solved in the present paper is not axisymmetrical. However, a certain generalization of the method which was applied in [2] permits construction of the exact solution of the problem at hand. It is assumed here that the surface of the crack has the form of a circular disk, i.e. that the velocity of propagation does not depend on direction. It is shown that, in general, this assumption is not borne out, but that it is possible to indicate a value of the initial stress for which the assumption is valid. For all other values of the initial stress the solution which is obtained can be considered as an approximate one.

1. Formulation of the problem. a) Two-dimensional case. A homogeneous and isotropic elastic medium having shear modulus μ and velocities of propagation of longitudinal and transverse waves a and b , respectively, fills an unbounded space and is in a state of homogeneous shear for $t < 0$, so that only one component of the stress tensor $\tau_{xz}^0 = \tau^0$ is nonzero. A crack forms at the instant $t = 0$ along the y -axis, and then propagates in the plane $z = 0$ in such a way that the elastic perturbations which arise from it do not depend on the coordinate y and are polarized in the xz plane. The velocity of propagation of the crack is assumed constant and is denoted by α . The location of the crack is shown in Fig.1. The shear stresses must disappear on the surface of the crack, i.e. the perturbations caused by the development of the crack must satisfy the condition

$$\tau_{xz} = -\tau^0 \text{ for } z = 0, |x| \leq \alpha t$$

Representation Theorem

$$\dot{u}_n(\mathbf{x}, t) = \frac{d}{dt} \left[\int_{-\infty}^{\infty} d\tau \iint_{\Sigma} s_i(\boldsymbol{\xi}, \tau) c_{ijpq} v_j \partial G_{np}(\mathbf{x}, t - \tau; \boldsymbol{\xi}, 0) / \partial \xi_q d\Sigma \right]$$

$s_i(\boldsymbol{\xi}, \tau)$: *The slip time function--discontinuity in slip across the fault.*

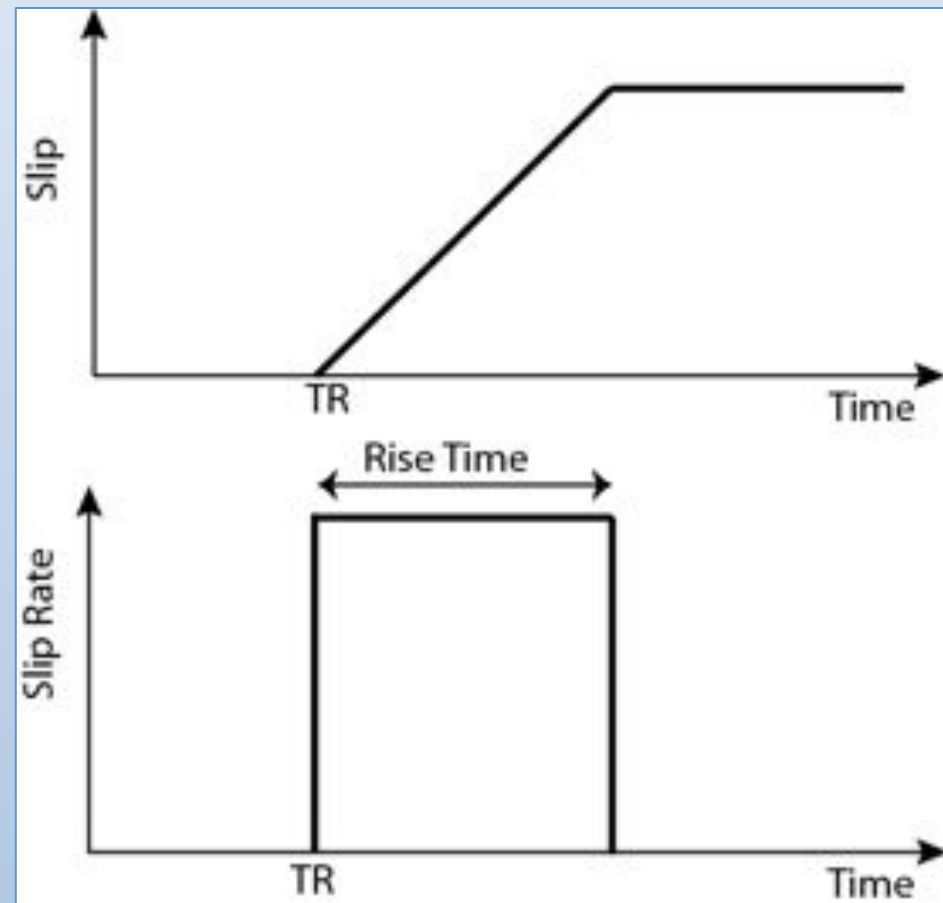
v_j : *Fault normal*

$\partial G_{np}(\mathbf{x}, t - \tau; \boldsymbol{\xi}, 0) / \partial \xi_q$: *Spatial derivative of the Green's function on the fault*

Note: Observed displacement is linearly related to slip.
Observed displacement is not linearly related to τ , time parameter

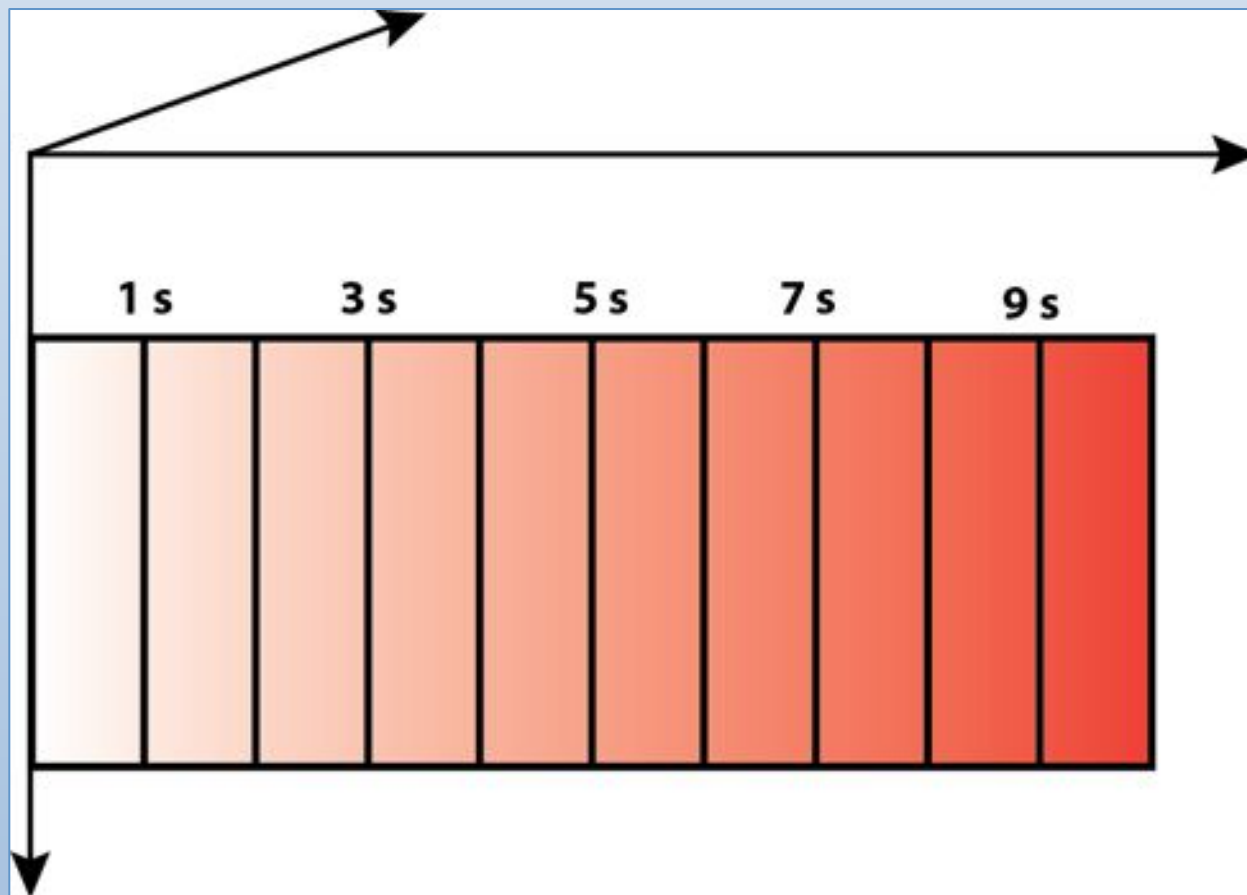
Finite Fault—Kinematic (Haskell, 1964)

- Fault Geometry: Length, Width
- Slip
- Rise Time
- Rupture Velocity



Haskell Model

Haskell Model: A rupture front propagates from one side of the fault at constant speed. Each point on the fault has the same slip and the same rise time. The time at which a point starts to slip is determined by the distance of that point from the hypocenter divided by the rupture speed. Basically propagation along a line.



Aki 1968

Seismic Displacements near a Fault

KIYUHI AKI

Department of Geology and Geophysics
Massachusetts Institute of Technology, Cambridge 02139

Ground motion at only 80 meters from the San Andreas fault was recorded during the Parkfield earthquake of June 28, 1966, by the accelerographs of the U. S. Coast and Geodetic Survey. Seismic displacements obtained from the accelerograms are compared with synthetic seismograms calculated for a moving dislocation model. An excellent agreement was obtained between the observed and theoretical seismograms. The dislocation is the only important source parameter that controls the seismic motion at such short distances. Other parameters such as the fault length and depth show negligible effect of the motion. The rupture velocity is a significant but not dominant factor. From the comparison of observed and theoretical seismograms, it was concluded that the fault dislocation was about 60 cm. This value is an order of magnitude greater than the fault offset observed at the surface. This discrepancy was attributed to the decoupling of a thin surface layer (probably less than 100 meters from the surface). The fault depth was estimated by combining the estimated dislocation with the seismic moment obtained from long-period surface waves. The fault depth within the basement rock was found to be about 3 km, which is significantly smaller than the depth (15 km) of the aftershock zone. This discrepancy was attributed to the effect of increasing friction with depth which momentarily prevented downward extension of rupture during the main shock.

INTRODUCTION

The recent Parkfield, California, earthquake (June 28, 1966, 04h 26m 14s GMT) offered an unprecedented opportunity for seismologists to study the seismic displacements near an earthquake fault. A strong motion seismograph operated by the Coast and Geodetic Survey [Cloud, 1966] recorded the seismic motion at only 80 meters from the San Andreas fault that moved during the earthquake.

In the present paper, we compared the actual seismic motion with the theoretical seismogram computed for a moving-dislocation model. For this earthquake, it was possible to construct such a model solely on the basis of field observations made during and after the earthquake by many geologists and seismologists. As a result of such a comparison, we are faced with an inconsistency between the strong motion data and a field observation with regard to the amount of dislocation. Additional information from long-period surface waves recorded at the World Wide Standard Seismic Network stations will be combined in an effort to obtain a unique picture of the earthquake source mechanism.

Our study will also be useful to earthquake

engineering, because it will link the geological data and the ground motion on the basis of a well-defined theoretical model of an earthquake.

Observed seismic displacement. Figure 1 is a map of the fracture zone associated with the Parkfield earthquake of June 28, 1966, based on the survey by Breen and Vedder [1967]. A main fracture zone 37 km long trends north-west-southeast. The fault movement was along a right-lateral strike slip of a few centimeters.

The fault trace cut across highway 46 near Cholame, where Allen and Smith [1966] observed, 10 hours following the main shock, that the white line on the road had been offset 4.5 cm in a right-lateral direction. The displacement increased during successive hours and days and reached about 11 cm a month later [Wallace and Roth, 1967]. The accelerograph station (designated as Station 2 in Cloud's report) operated by the Coast and Geodetic Survey is located very close to this point. The three component records obtained there are reproduced in Figure 2 from a report by Cloud [1966].

Unfortunately, the accelerograph sensitive to the direction parallel to the fault strike was

Haskell 1969

ELASTIC DISPLACEMENTS IN THE NEAR-FIELD OF A PROPAGATING FAULT

By N. A. HASKELL

ABSTRACT

Displacement, particle velocity, and acceleration wave forms in the near field of a propagating fault have been computed by numerical integration of the Green's function integrals for an infinite medium. The displacement discontinuity (dislocation) on the fault plane is assumed to have the form of a unilaterally propagating finite ramp function in time. The calculated wave forms in the vicinity of the fault plane are quite similar to those observed at the strong motion station nearest the fault plane at the Parkfield earthquake. The comparison suggests that the propagating ramp time function is roughly representative of the main features of the dislocation motion on the fault plane, but that the actual motion has somewhat more high frequency complexity. Calculated amplitudes indicate that the average final dislocation on the fault at the Parkfield earthquake was more than an order of magnitude greater than the offsets observed on the visible surface trace. Computer generated wave form plots are presented for a variety of locations with respect to the fault plane and for two different assumptions on the relation between fault length and ramp function duration.

INTRODUCTION

In view of current programs for the extensive installation of close-in instrumentation along known active faults it seems likely that in the future we shall have increasing quantities of data from areas in the immediate neighborhood of shallow earthquake sources. A noteworthy example has already been obtained from the Cholame-Shandon strong-motion array of the U. S. Coast and Geodetic Survey and the California Department of Water Resources during the Parkfield, California earthquake of 28 June 1966, where Station 2 of the array was located about 80 meters from the visible surface trace of the fault (Morrison, Hofmann and Wolfe, 1966; Cloud and Perez, 1967). It seems timely, therefore, to give some preliminary consideration to the distribution of displacements, particle velocities, and accelerations to be expected in the near field of a source model that will, in some measure, simulate the propagation of a fracture over a fault plane.

The elastodynamic representation theorem in the form given by de Hoop (1958) provides the mathematical basis for such a calculation. A form of this theorem appropriate for the representation of a faulting source in an infinite homogeneous medium has been given in a previous paper (Haskell, 1964) as follows:

$$u_i(x, t) = - \iint_S \{ \rho(\alpha^2 - 2\beta^2)n_j M_{ij, \alpha} [D_j] + \rho\beta^2(n_j M_{ij, \beta} [D_j] + n_p M_{ip, \alpha} [D_p]) \} dS \quad (1)$$

The notation is:

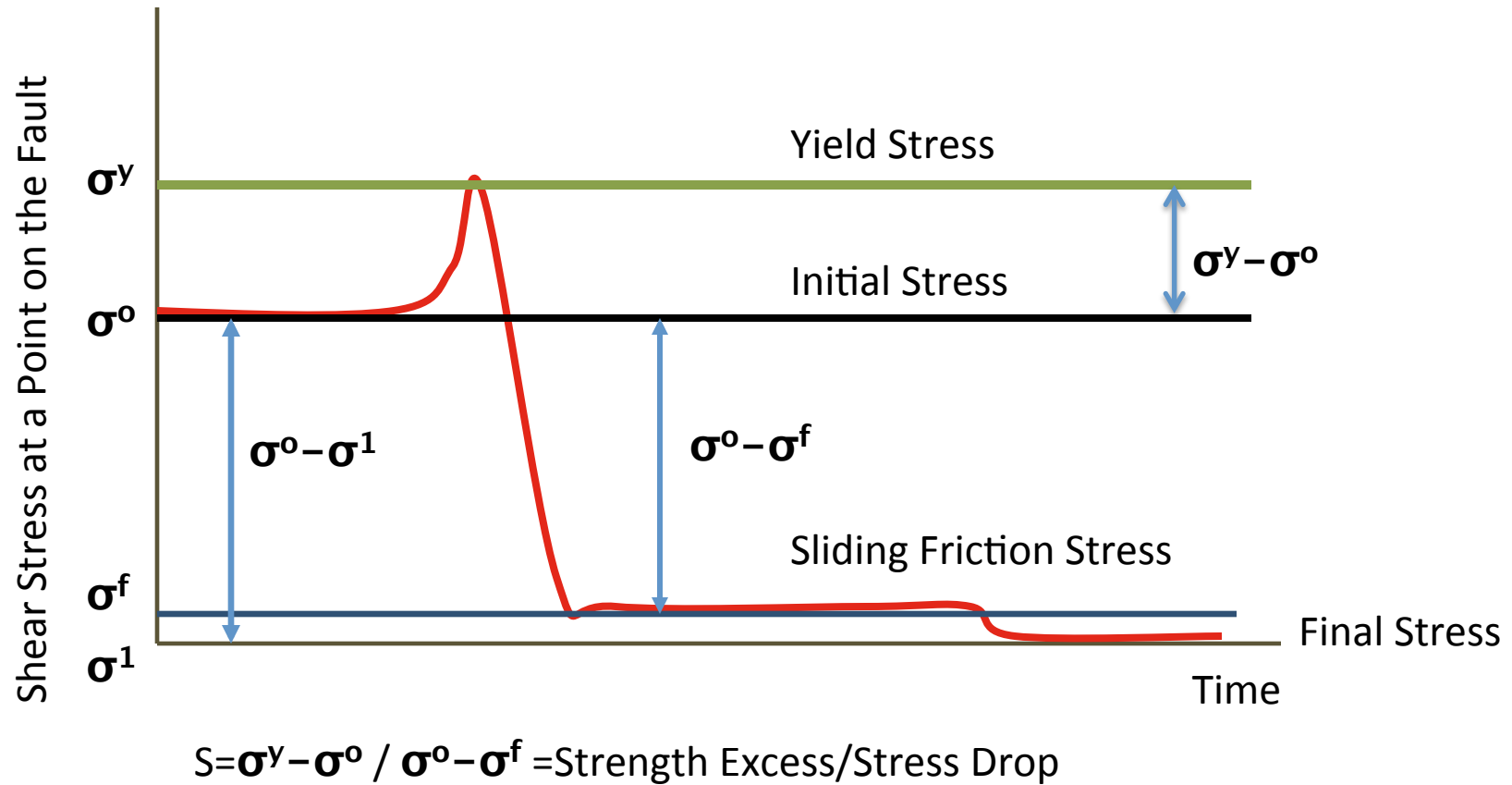
S = Fault plane area,

$\mathbf{u} = (u_1, u_2, u_3)$ = Cartesian components of displacement measured from the initial state. (Printed as capitals in Figures from computer output.)

Rupture Dynamics

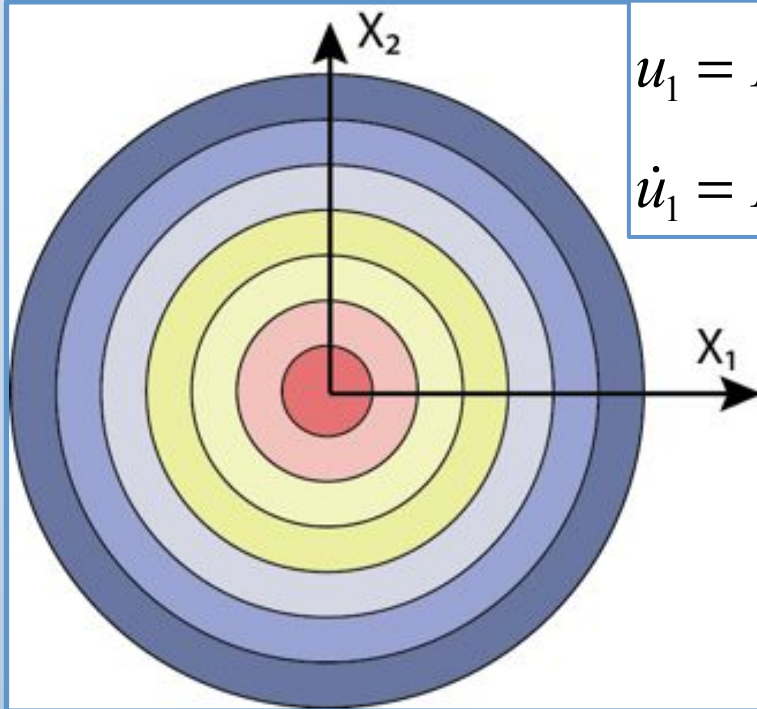
- **Stresses: yield, initial, sliding friction and in some cases, the absolute value of friction.**
- **Constitutive law for friction**
- **Fault geometry**

Stress at a point on the fault



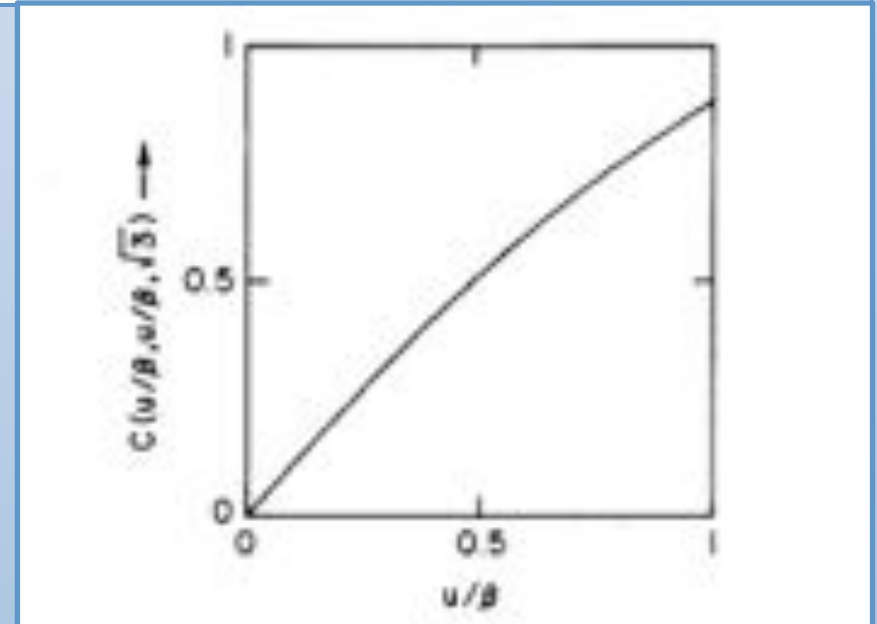
Kostrov Dynamics (1964)

The shear stress σ_{31} is released by an outward expanding circular rupture (0.85β).



$$u_1 = H(t - x_1 / v) c(v / \beta) (\sigma_E / \mu) \beta \sqrt{t^2 - (x_1 / v)^2}$$

$$\dot{u}_1 = H(t - x_1 / v) c(v / \beta) (\sigma_E / \mu) \beta t / \sqrt{t^2 - (x_1 / v)^2}$$



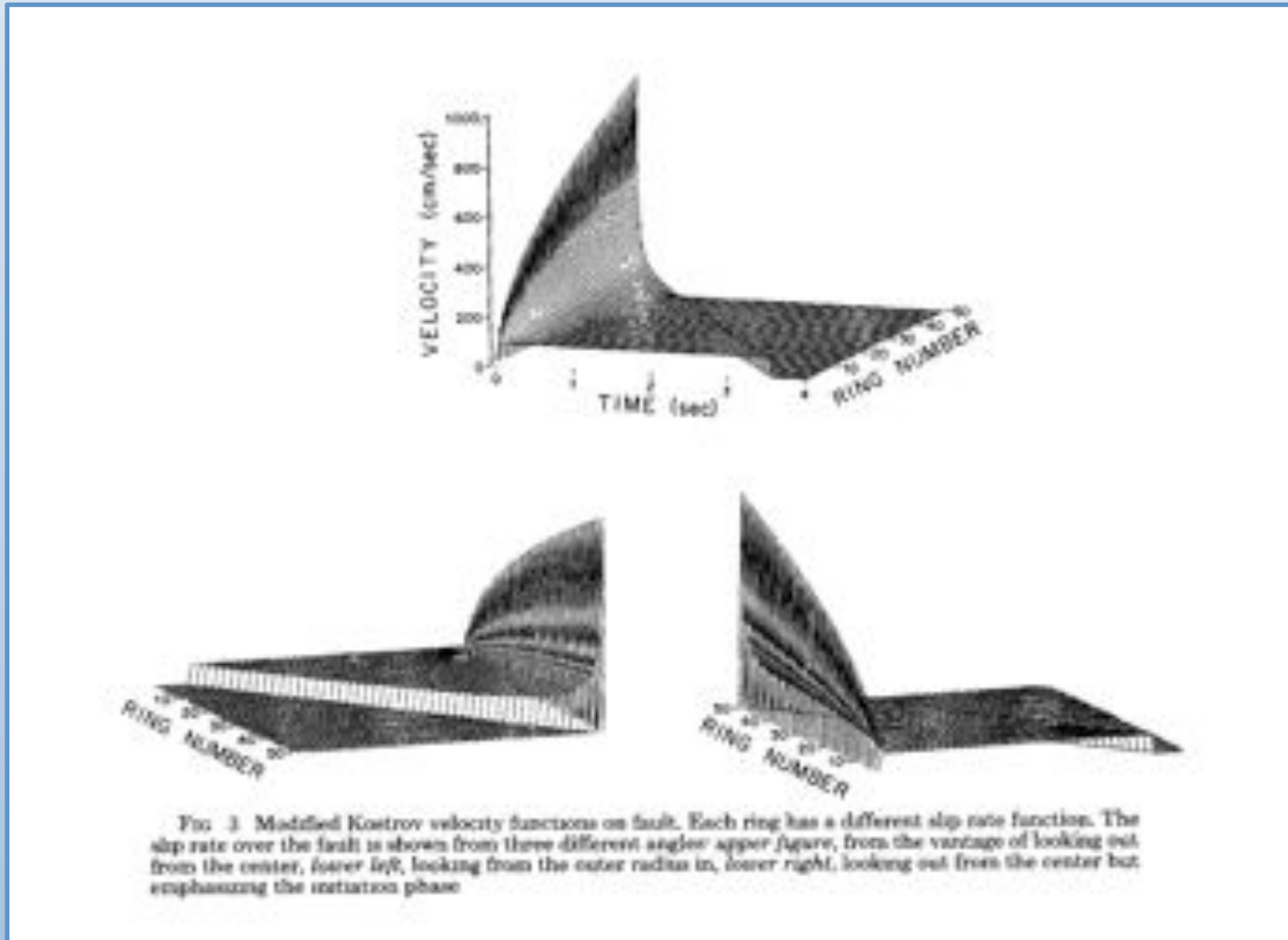
$c(v/\beta)$ is close to v/β for $v/\beta > 0.5$

Kostrov Slip Rate

$$\dot{s}(r, t) = C(v / \beta) \left(\frac{\sigma_E}{\mu} \right) \left(\frac{\beta t H(t - r/v)}{\sqrt{t^2 - (r/v)^2}} \right)$$

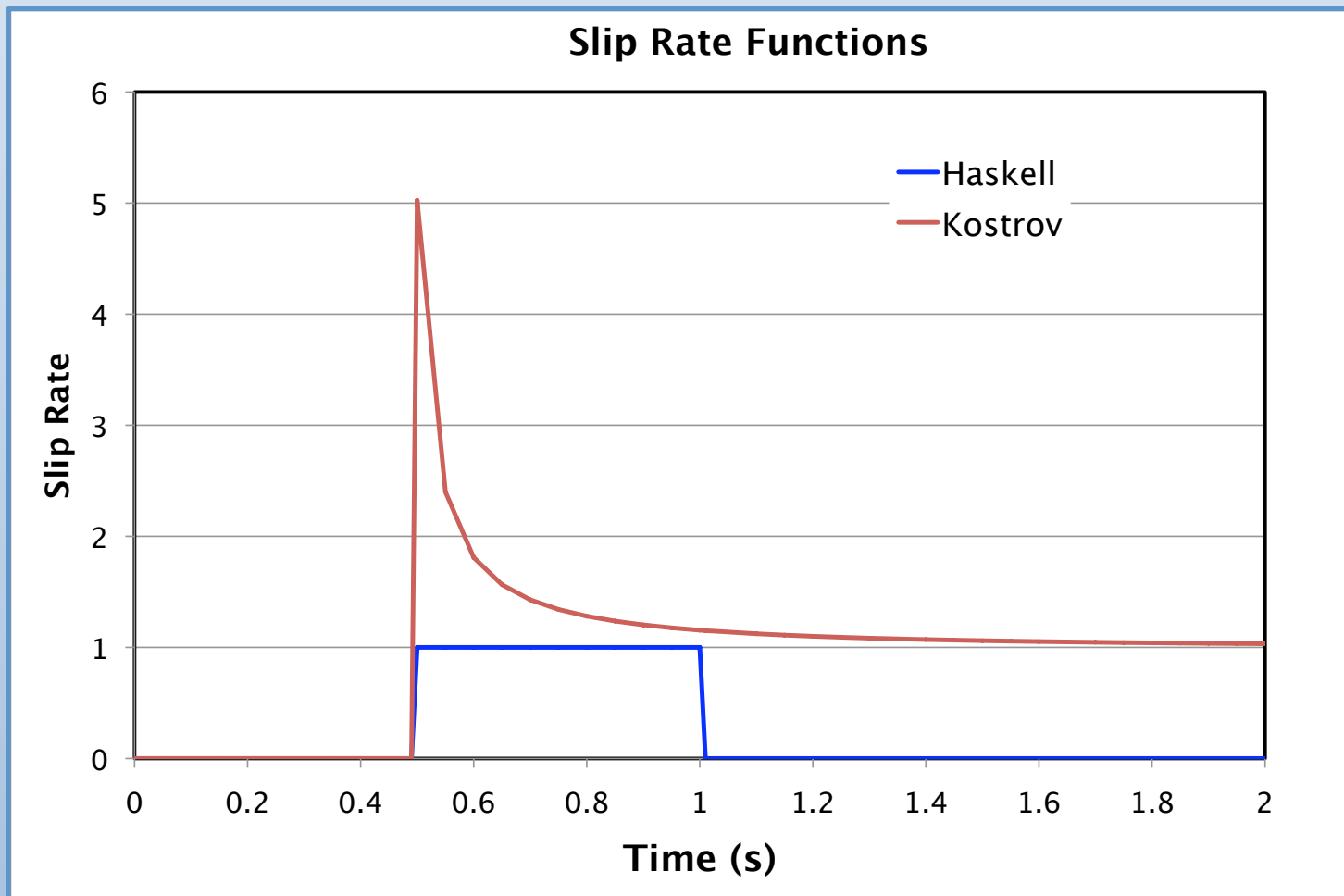
1. What is the value at $r=0$?
2. What is the value at $r=R$ and t going to infinity?
3. What is its Fourier amplitude spectrum?

Kostrov Slip Rate



Haskell & Kostrov Slip Rate

The farfield (which contributes most of the ground motion even in the near-source region) displacement amplitude is proportional to the slip rate on the fault.



Haskell: $du / dt \propto \int \ddot{s}$

$$u_i(\mathbf{x}, t) = - \iint_{S^+} \left\{ \rho(\alpha^2 - 2\beta^2)n_j^+ M_{ij,kl}[D_k] + \rho\beta^2(n_i^+ M_{ij,kl}[D_k] + n_j^+ M_{ij,kl}[D_k]) \right\} ds \quad (7)$$

where the operator $M_{ij,kl}$ is defined by

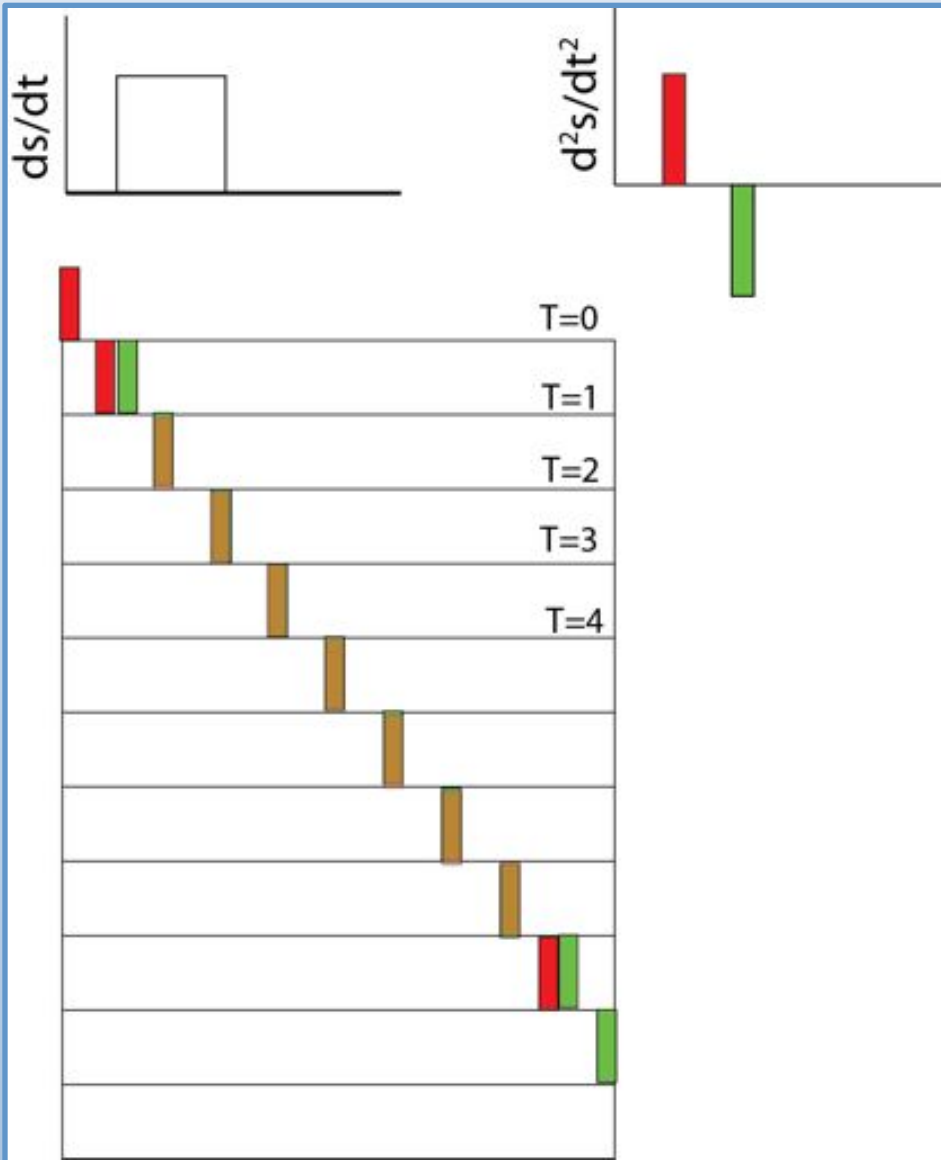
$$M_{ij,kl}[\varphi(\xi, t)] = (4\pi\rho)^{-1} \left\{ [15\gamma_i \gamma_j \gamma_k - 3(\delta_{ij} \gamma_k + \delta_{ik} \gamma_j + \delta_{jk} \gamma_i)] r^{-3} \cdot \int_{r/\alpha}^{r/\beta} \dot{\varphi}(\xi, t - \ell) \ell' d\ell + [6\gamma_i \gamma_j \gamma_k - (\delta_{ij} \gamma_k + \delta_{ik} \gamma_j + \delta_{jk} \gamma_i)] (\alpha r)^{-2} \varphi(\xi, t - r/\alpha) - [6\gamma_i \gamma_j \gamma_k - (2\delta_{ij} \gamma_k + \delta_{ik} \gamma_j + \delta_{jk} \gamma_i)] (\beta r)^{-2} \varphi(\xi, t - r/\beta) + \gamma_i \gamma_j \gamma_k (\alpha^3 r)^{-1} \dot{\varphi}(\xi, t - r/\alpha) - [\gamma_i \gamma_j \gamma_k - \delta_{ij} \gamma_k] (\beta^3 r)^{-1} \dot{\varphi}(\xi, t - r/\beta) \right\} \quad (8)$$

The dot superscript is used to indicate the time derivative.

If we define the radiated energy of a source as that energy that would be transmitted to infinity if the given source were embedded in an infinite, lossless medium, the only terms of equations (7) and (8) that are relevant in computing that energy are the far-field terms that are proportional to r^{-2} that is, those resulting from the last two terms in equation (8). Carrying out the substitution and taking the time derivative we obtain for the particle velocity, \dot{u}_i ,

$$4\pi\dot{u}_i(\mathbf{x}, t) = - \iint_{S^+} (\alpha r)^{-1} [(1 - 2(\beta/\alpha)^2)\gamma_i n_j^+ + 2(\beta/\alpha)^2 \gamma_i \gamma_j \gamma_k n_k^+] \dot{D}_j(\xi, t - r/\alpha) ds + \iint_{S^+} (\beta r)^{-1} [2\gamma_i \gamma_j \gamma_k n_k^+ \dot{D}_j(\xi, t - r/\beta) - \gamma_k (n_k^+ \dot{D}_j(\xi, t - r/\beta) + n_i^+ \dot{D}_k(\xi, t - r/\beta))] ds \quad (9)$$

Haskell: No Radiation Except at Start and End



In Haskell's model, which has a boxcar shape for the slip rate function, the only radiation comes from the start and end. This presumes two important features of the faulting:

- 1) Constant slip rate at every point.
- 2) Constant rupture velocity.

Representation Theorem

$$\dot{u}_n(\mathbf{x}, t) = \frac{d}{dt} \left[\int_{-\infty}^{\infty} d\tau \iint_{\Sigma} s_i(\boldsymbol{\xi}, \tau) c_{ijpq} v_j \partial G_{np}(\mathbf{x}, t - \tau; \boldsymbol{\xi}, 0) / \partial \xi_q d\Sigma \right]$$

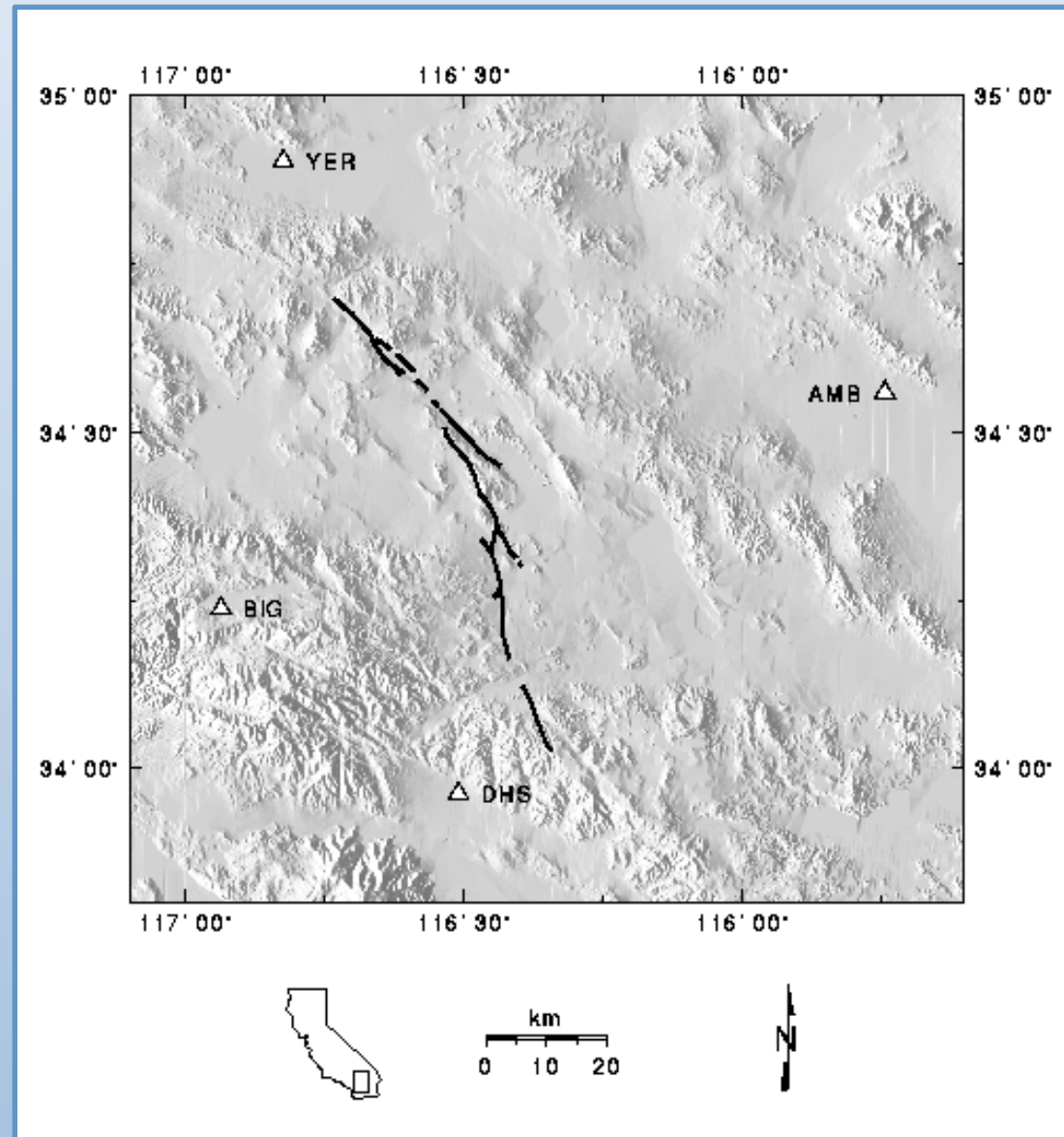
$s_i(\boldsymbol{\xi}, \tau)$: *The slip time function--discontinuity in slip across the fault.*

v_j : *Fault normal*

$\partial G_{np}(\mathbf{x}, t - \tau; \boldsymbol{\xi}, 0) / \partial \xi_q$: *Spatial derivative of the Green's function on the fault*

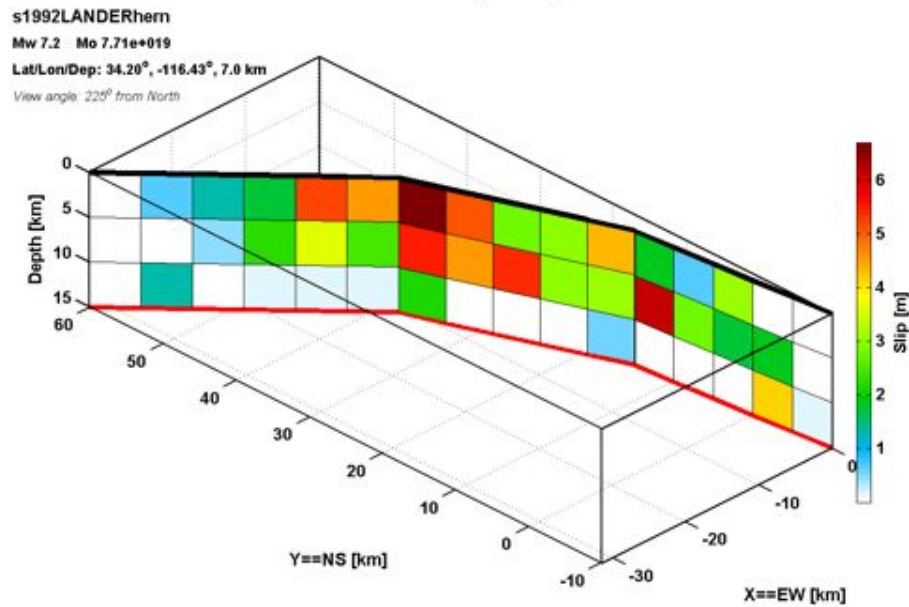
Note: Observed displacement is linearly related to slip.
Observed displacement is not linearly related to τ , time parameter

Map of Landers Surface Rupture

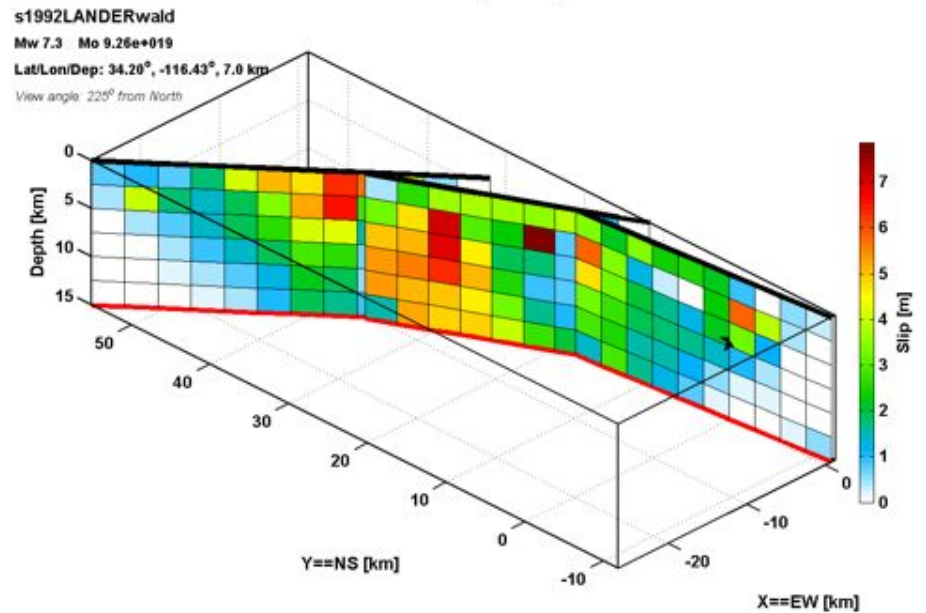


Slip Distributions for Landers

Landers (Calif.)



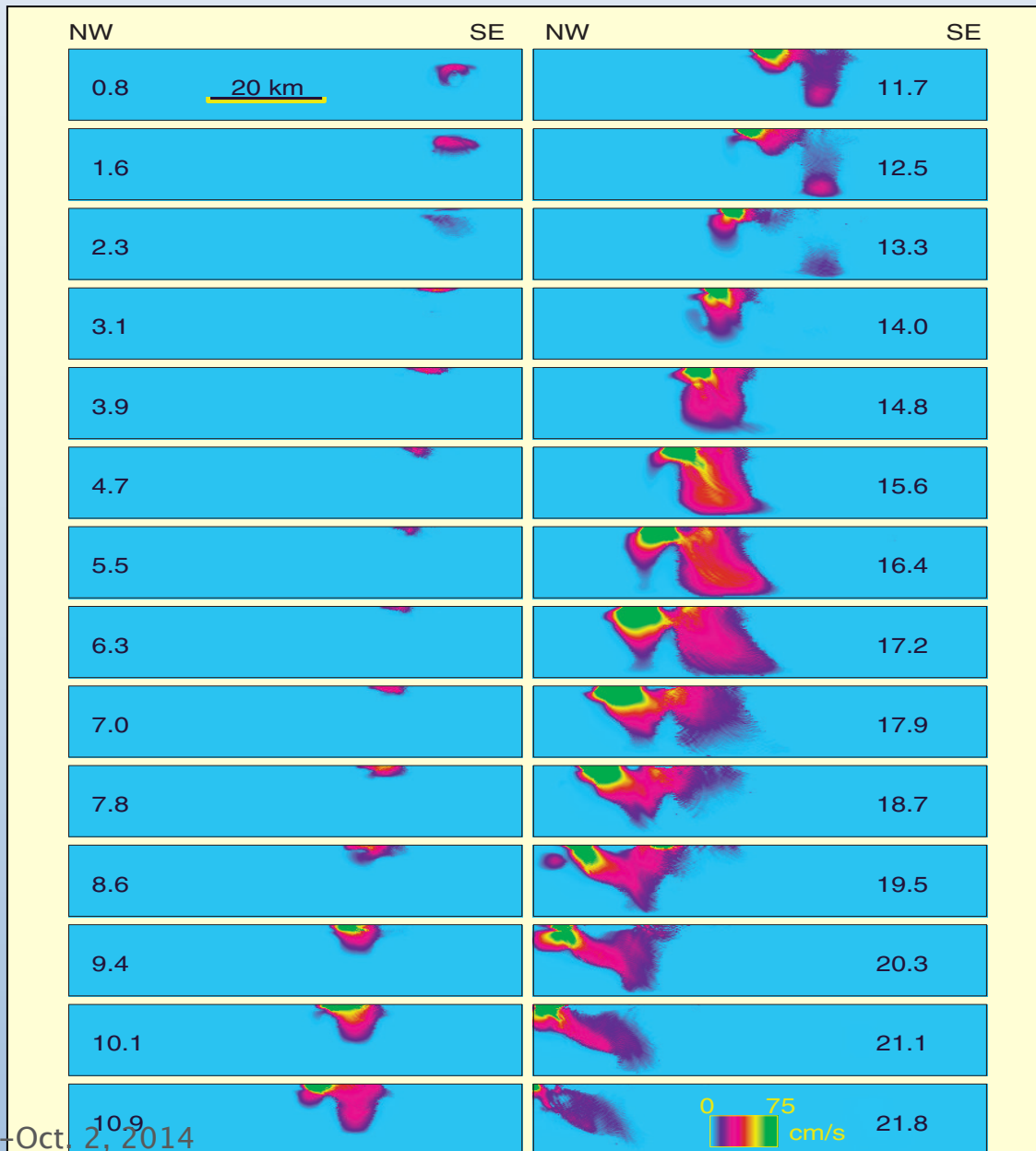
Landers (Calif.)



Hernandez et al. (1999)

Wald and Heaton (1994)

Images of Sliprate during Landers Simulation

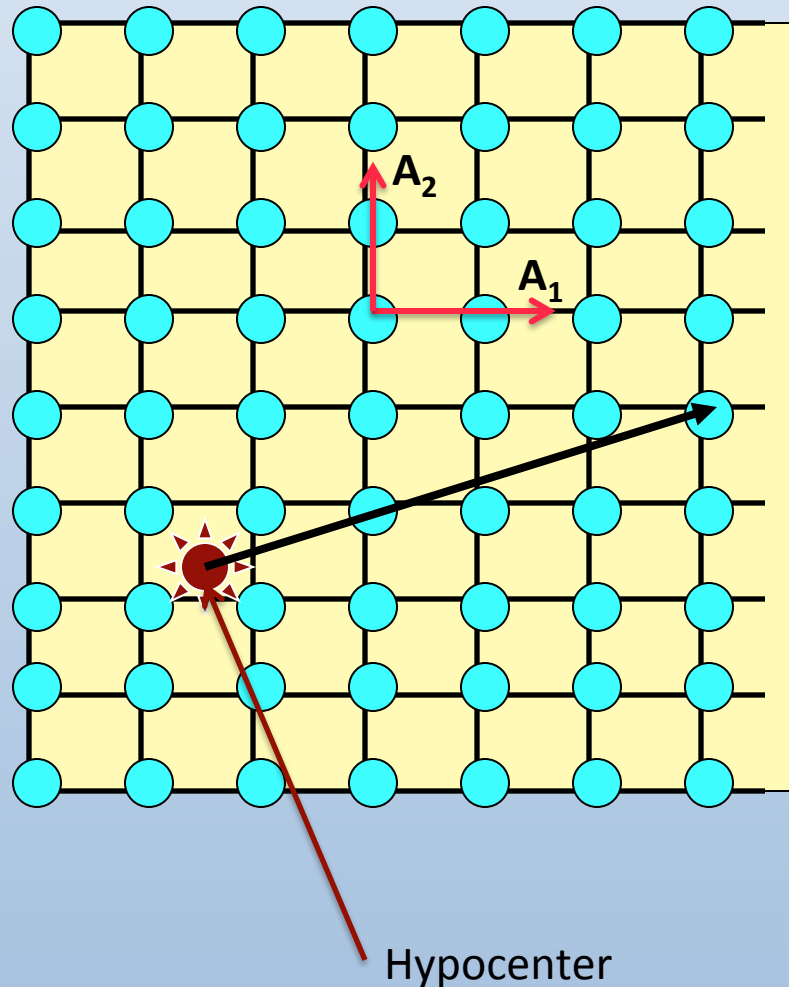


Snapshots of slip rate at 1 s intervals

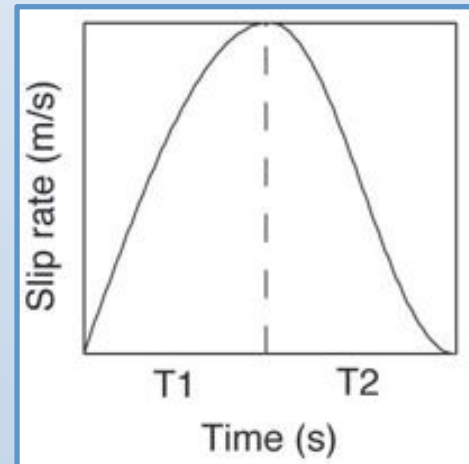
Intensity of the color is related to slip rate

Olsen, Madariaga, Archuleta, Science 1997

Kinematic Source Parameters



Slip rate time function

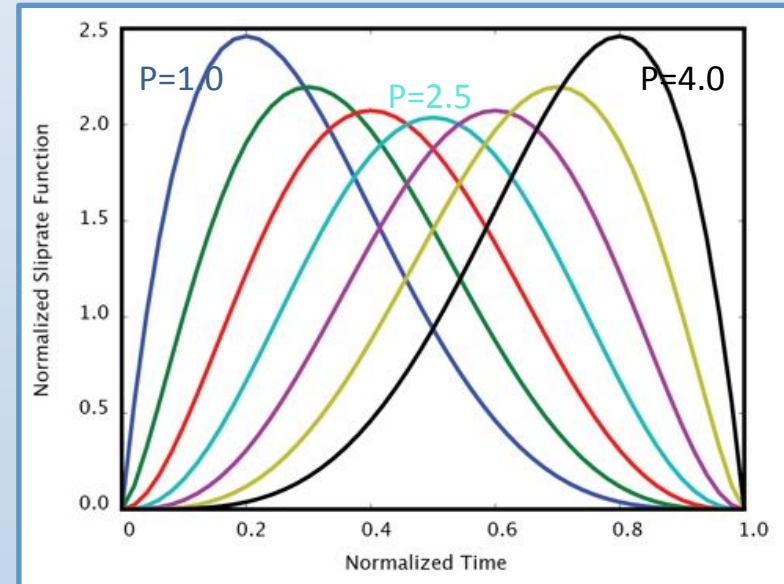
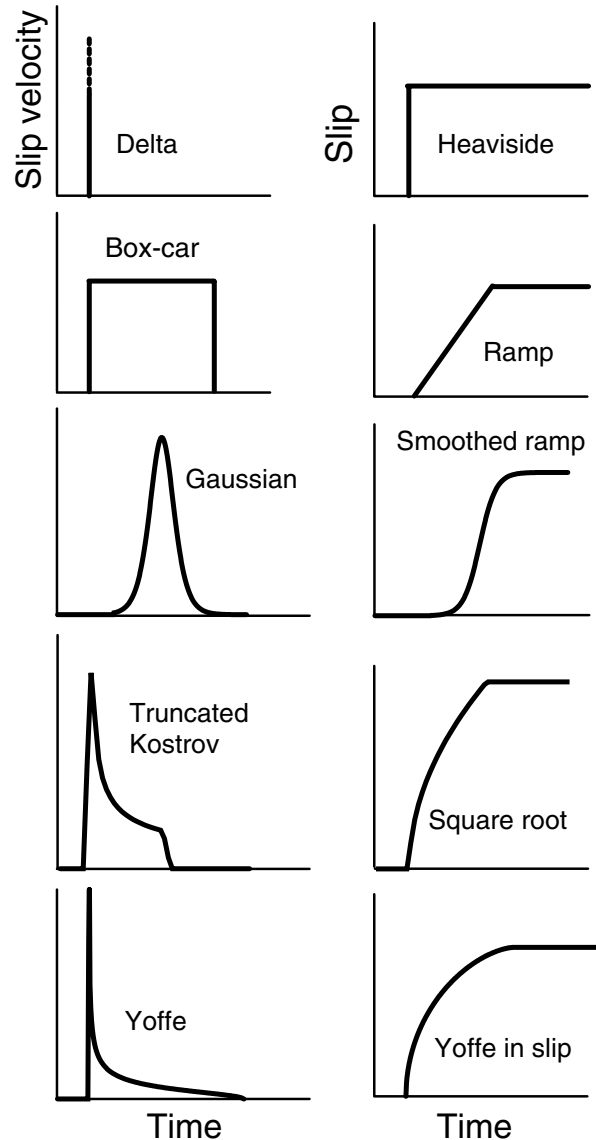


Source parameters:

- Slip amplitude (A_1 , A_2)
- Rupture velocity
- Rise time function (T_1 , T_2 , ...)
- Geometry (L , W , δ)
- Hypocenter

Sliprate Function

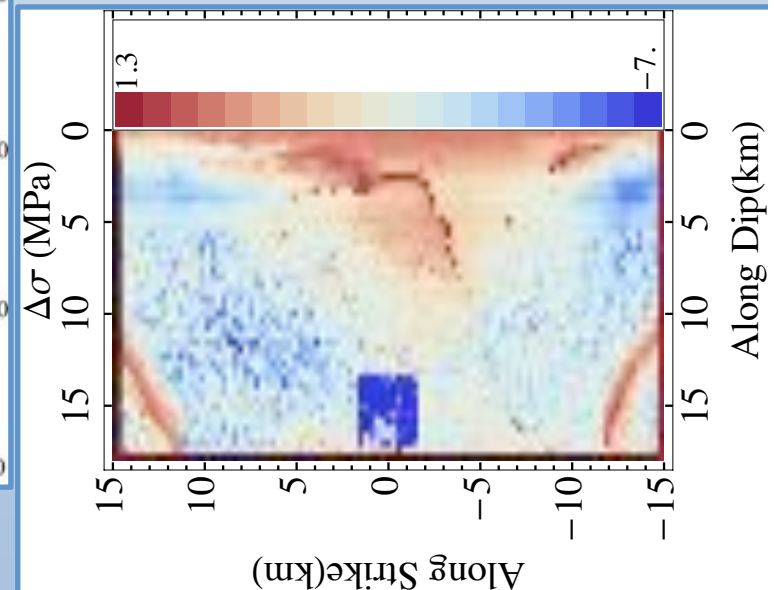
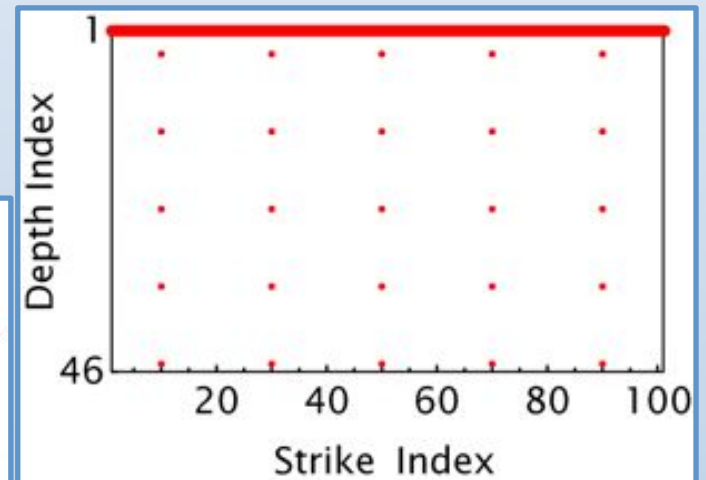
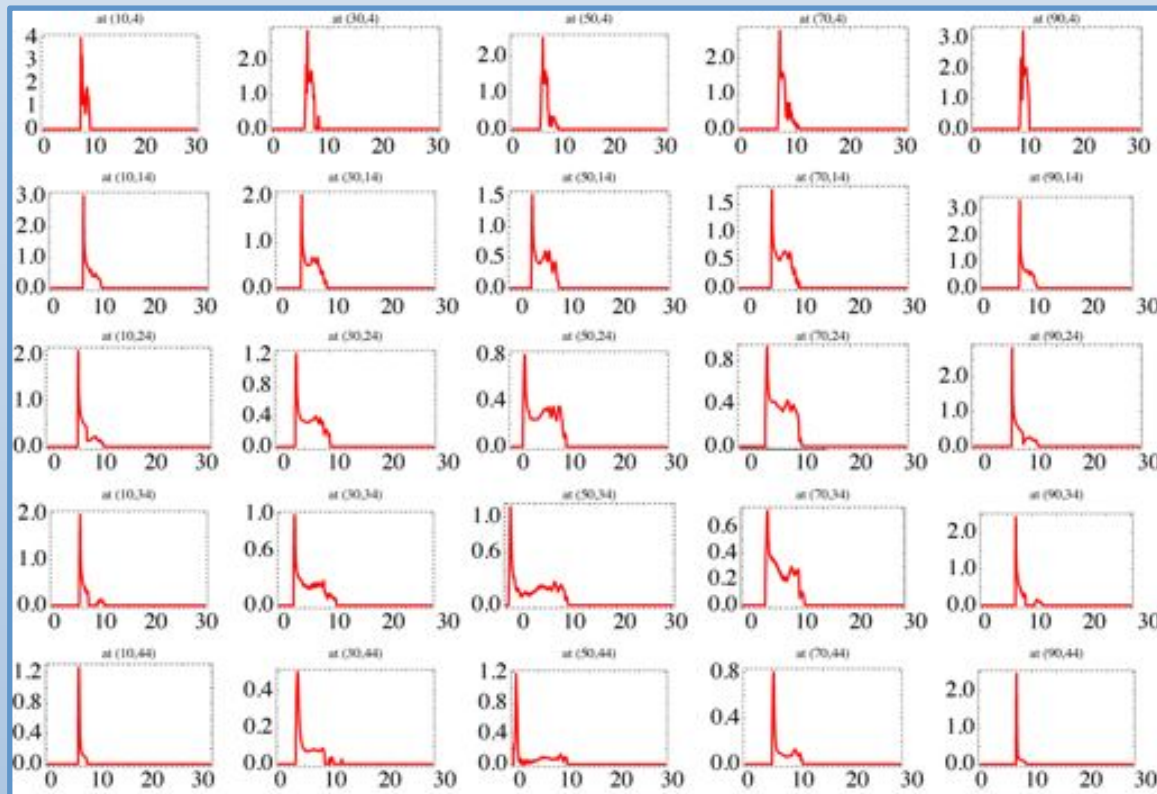
E. Tinti, E. Fukuyama, A. Piatanesi, and M. Cocco



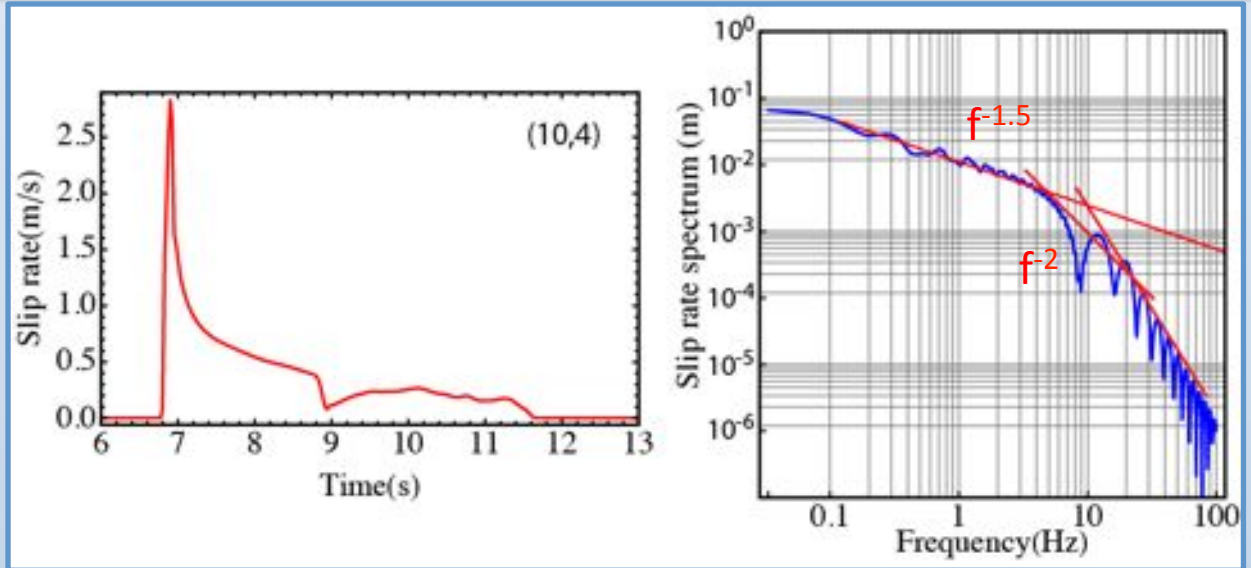
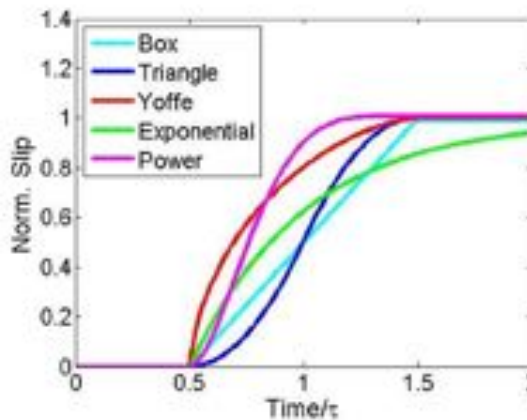
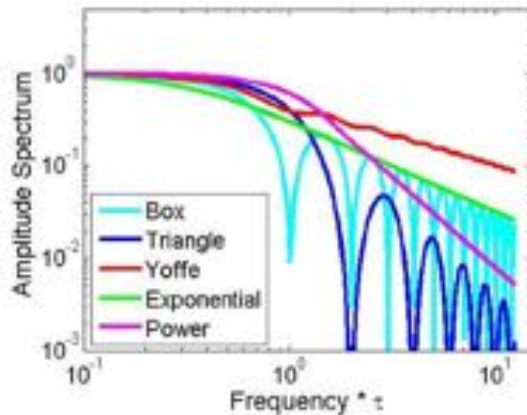
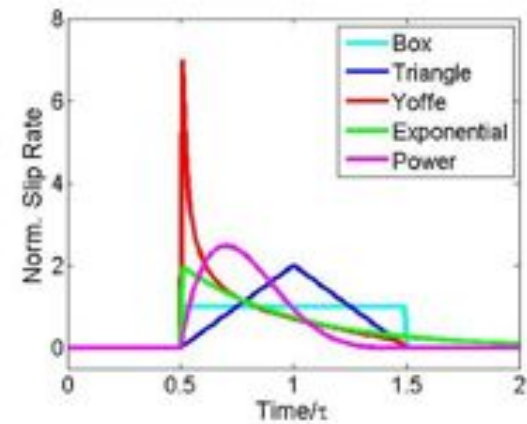
$$\dot{s}(\xi, t) = C \left(\frac{t}{T_r} \right)^p \left(1 - \frac{t}{T_r} \right)^{5-p}$$

Liu and Archuleta, JGR, 2004

Sliprate Functions: Dynamic Rupture



Sliprate Spectra



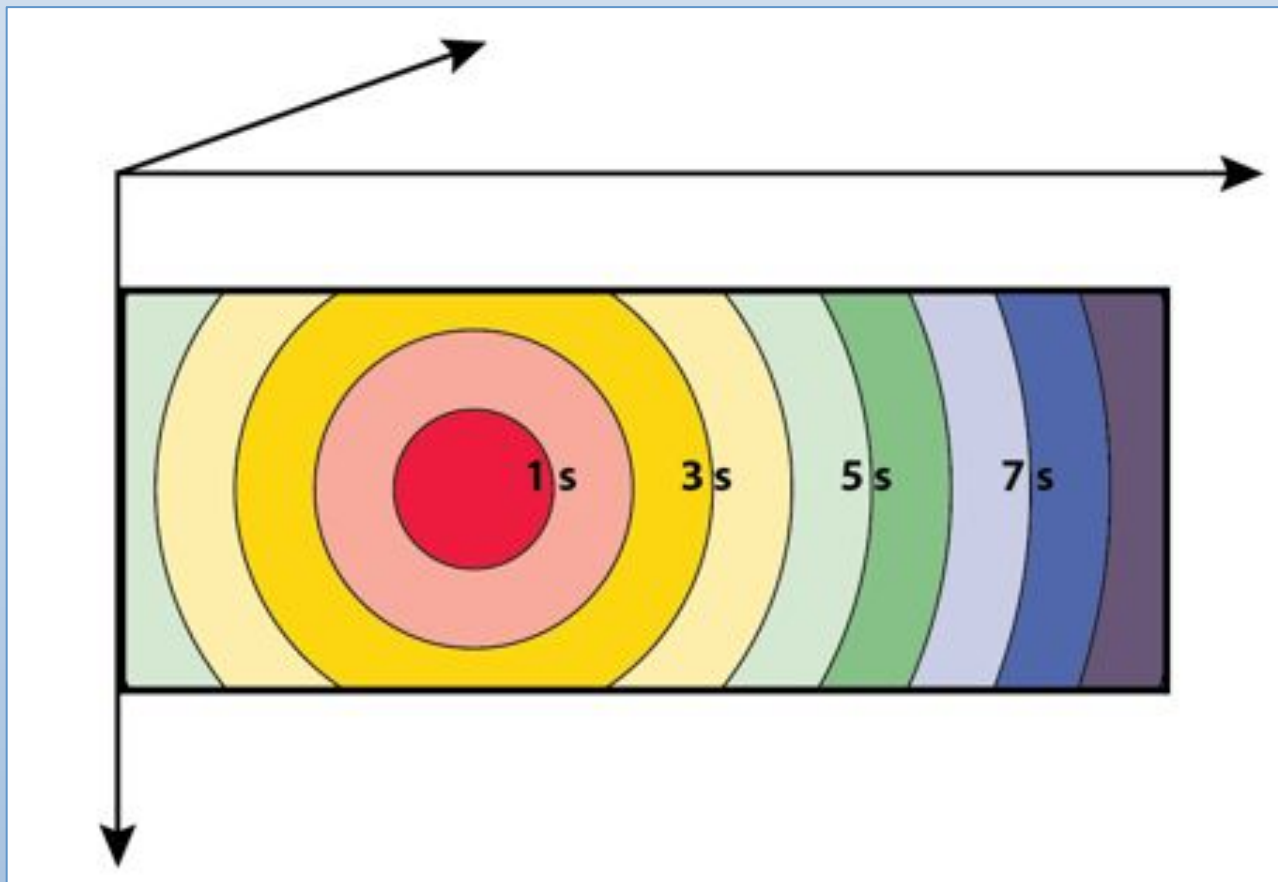
Results from dynamic rupture, normal fault, Q. Liu, 2013

Festa and Zollo, 2012

In The Mechanics of Faulting: From Laboratory to Real Earthquakes

Constant Rupture Velocity

A rupture front radiates out from the hypocenter at constant speed. For Haskell each point on the fault has the same slip and the same rise time. The time at which a point starts to slip is determined by the distance of that point from the hypocenter divided by the rupture speed.



Landers Dynamic Rupture



Olsen, Madariaga,
Archuleta, Science 1997

TOTAL ENERGY AND ENERGY SPECTRAL DENSITY OF ELASTIC WAVE RADIATION FROM PROPAGATING FAULTS. PART II. A STATISTICAL SOURCE MODEL.

By N. A. HASKELL

ABSTRACT

Previously derived expressions for the total energy and energy spectral density of elastic waves radiated by a propagating fault are rewritten in terms of a spacio-temporal autocorrelation of the acceleration of relative displacement over the fault plane. This is interpreted in a statistical sense as the average autocorrelation over an ensemble of earthquakes. An explicit form of autocorrelation function is assumed, depending upon two parameters, a correlation length, and a correlation time, and the total energy and energy spectral density are derived in terms of these parameters. By using scaling laws due to Bath and Duda for earthquake volume and radiation efficiency as functions of magnitude, the statistical parameters may also be related to magnitude.

INTRODUCTION

In a previous paper (Haskell 1964), hereafter referred to as Part I, expressions for the total *P* and *S* wave energies and the corresponding spectral density distributions were derived on the basis of a deterministic source model. That is, the relative displacement between opposite faces of the fault plane was taken to be a definitely specified function of time and the spacial coordinates in the fault plane. It was pointed out that such a model was probably unrealistic, since the actual spacial and temporal dependence of the fault displacement was likely to be far too complex to be represented by any simply specifiable mathematical function, and it was suggested that it would be desirable to develop a model in which the source was described in statistical rather than deterministic terms. Engineering seismologists, dealing with the highly irregular ground motions observed on strong-motion instruments at short epicentral distances, have found that the general characteristics of the observed acceleration can be well represented by considering the source to be a random sequence of short impulses (Housner, 1947, 1955; Thomson 1959). Although the high frequency motions observed in the epicentral region are relatively rapidly attenuated and contribute little to the signal observed at teleseismic distances, they may represent a significant part of the total elastic wave energy radiated by the earthquake and must be accounted for by any satisfactory conceptual model of the earthquake source.

In Part I, the radiated energy was expressed in terms of certain integrals, $\int_{-\infty}^{+\infty} I_p^2 dt$ for *P* waves and $\int_{-\infty}^{+\infty} I_s^2 dt$ for *S* waves, where

$$I_p = \int_{-\infty}^{+\infty} \ddot{D}(\xi, t - r/a) d\xi; \quad (1)$$

Haskell 1966

SOURCE AUTOCORRELATION FUNCTION

Since we shall have to choose a particular form for the ensemble average $\Phi(\eta, \epsilon)$ on a more or less intuitive basis, it is of some interest to see what this function looks like for a particular deterministic model. For this purpose we consider the modulated ramp displacement function that was treated in Part I. In this case

$$\begin{aligned} \ddot{D}(\xi, t) &= D_0(2\pi v/T^2) \sin(2\pi v|t - \xi/v|/T), & 0 < t - \xi/v < T, \\ &= 0, & (t - \xi/v) < 0 \text{ or } > T, \end{aligned} \quad (9)$$

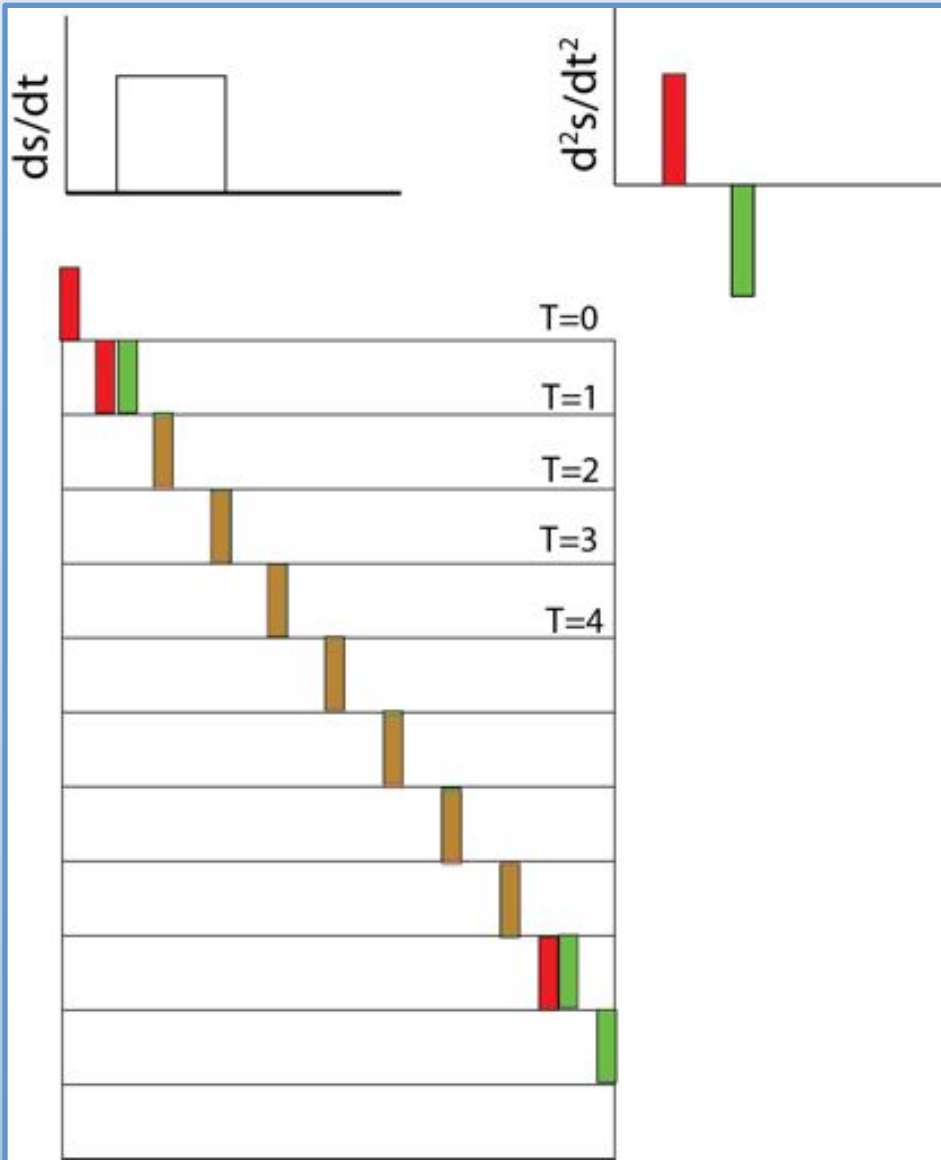
where D_0 is the final displacement on the fault, T is the duration of the fault motion at a fixed point, v is the fault propagation velocity, and n is an integer. For this function we find by direct integration of equation (2)

$$\begin{aligned} \Phi(\eta, \epsilon) &= (2\pi^2 v^2 L D_0^2 / T^2) (1 - |\eta|/L) [1 - |\epsilon - \eta/v|/T] \cos(2\pi n|\epsilon - \eta/v|/T) \\ &\quad + (2\pi n)^{-1} \sin(2\pi n|\epsilon - \eta/v|/T), & \text{for } |\eta| \leq L \text{ and } |\epsilon - \eta/v| \leq T, \\ &= 0, & \text{for } |\eta| > L \text{ or } |\epsilon - \eta/v| > T. \end{aligned} \quad (10)$$

It will be noted that Φ is expressed as a product of a spacial factor which depends on $|\eta|$ alone and a spacio-temporal factor which depends on both time and space lags in the form $|\epsilon - \eta/v|$. The spacial factor is a linear decrease from 1 at $\eta = 0$ to zero at $|\eta| = L$. The spacio-temporal factor is plotted in Figure 1 for the case $n = 3$.

In contrast to equation (9), which represents a fixed wave-form propagating unchanged along the fault, we visualize the actual progress of faulting as a swarm of acceleration and deceleration pulses that propagates along the fault as a group with a mean velocity, v , but which is highly chaotic in detail. We assume that the velocity, v , is common to all members of the ensemble and that the ensemble average of Φ can still be factored into a product of a function of $|\eta|$ and a function of $|\epsilon - \eta/v|$. In choosing an explicit form for these factors we note that a great many

Haskell: No Radiation Except at Start and End



In Haskell's model, which has a boxcar shape for the slip rate function, the only radiation comes from the start and end. This presumes two important features of the faulting:

- 1) Constant slip rate at every point.
- 2) Constant rupture velocity.

Representation Theorem

$$\hat{\mathbf{a}} \cdot \ddot{\mathbf{u}}^s = \ddot{f}_r * \int_{\mathbf{y}(t,\mathbf{x})} \left[c^2 \left(\frac{d\mathbf{s}_r}{dq} \cdot \mathbf{G}_a^s \right) + c^2 \left(\frac{d\mathbf{G}_a^s}{dq} \cdot \mathbf{s}_r \right) + \frac{dc}{dt} (\mathbf{s}_r \cdot \mathbf{G}_a^s) \right] dl$$

*Slip Rate
Time Function*

*Stress Drop
(spatial derivative of slip)*

*Change in isochrone
velocity--acceleration
of the the rupture front*

Spudich and Frazer, BSSA, 1984
Bernard and Madariaga, BSSA, 1984

1- and 2-Point Statistics

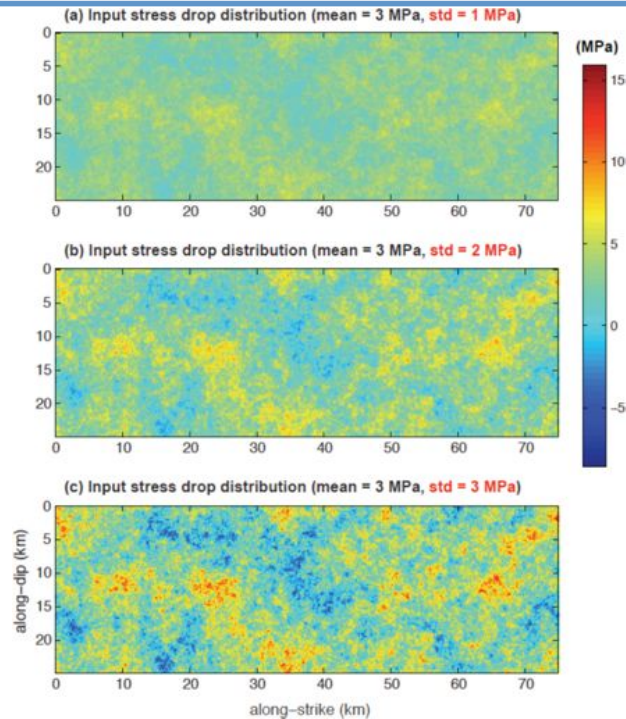


Figure 5. Input stress drop distribution with the same Gaussian 1-point statistics, but different standard deviations, that is (a) 1 MPa, (b) 2 MPa, (c) 3 MPa. All three distributions have the same mean stress drop ($=3$ MPa) and follow the same spectral decay rate (k^{-1}).

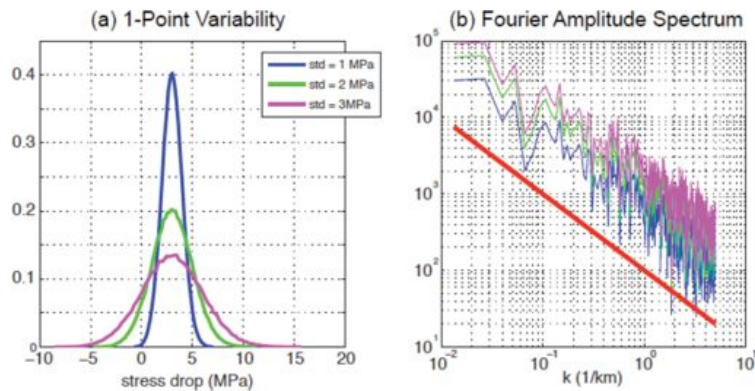


Figure 6. 1-point probability density function (a) and Fourier amplitude spectrum (b) of three input stress drop distributions in Fig. 5. Note that they all have the same spectral decay rate (k^{-1}) although the standard deviation varies from 1 to 3 MPa. The red solid line in (b) shows a reference spectral decay rate (k^{-1}).

ESE 10 - 4 MAI AND BEROZA: RANDOM FIEL

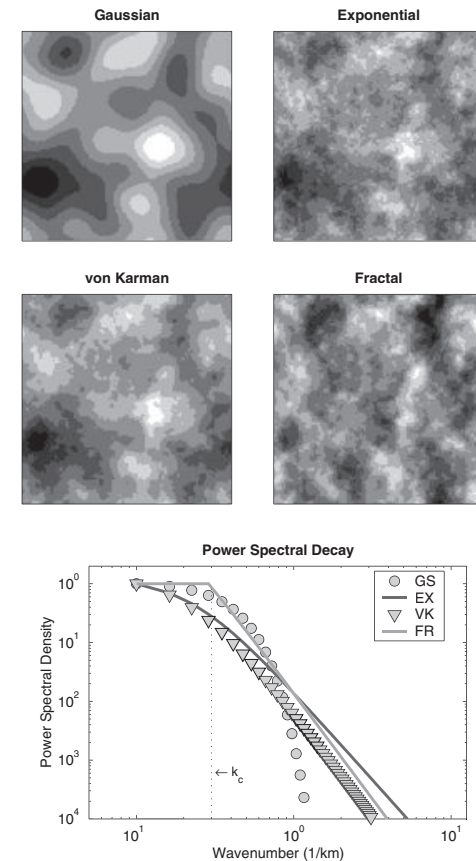
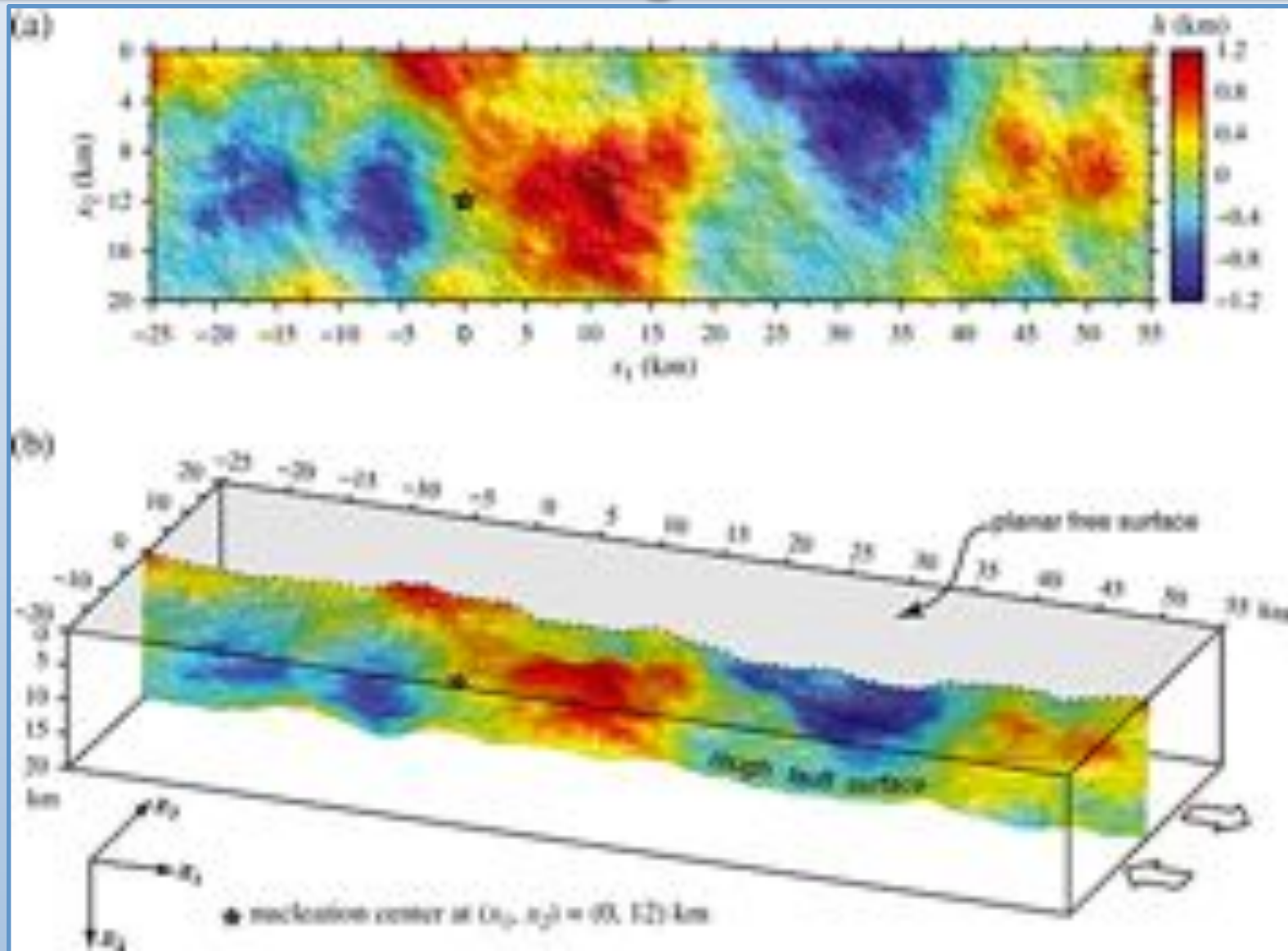


Figure 2. Examples of the spatial random field models considered in this study, generated with identical phasing to facilitate the comparison. The grid dimensions are 30×30 km; the correlation lengths are $a = 5$ km for the Gaussian, exponential, and von Karman ACF. For the von Karman model, $H = 0.8$; for the fractal case, $D = 2.2$ and $k_c = 0.3$. The bottom graph displays the corresponding power spectral decays of a one-dimensional slice (at $k_z = 0$) of the two-dimensional power spectrum $P(k)$.

Shi and Day: Rupture Dynamics and Ground Motion from 3-D Rough-Fault Simulations



Journal of Geophysical Research: Solid Earth

Volume 118, Issue 3, pages 1122-1141, 31 MAR 2013 DOI: 10.1002/jgrb.50094

<http://onlinelibrary.wiley.com/doi/10.1002/jgrb.50094/full#jgrb50094-fig-0001>

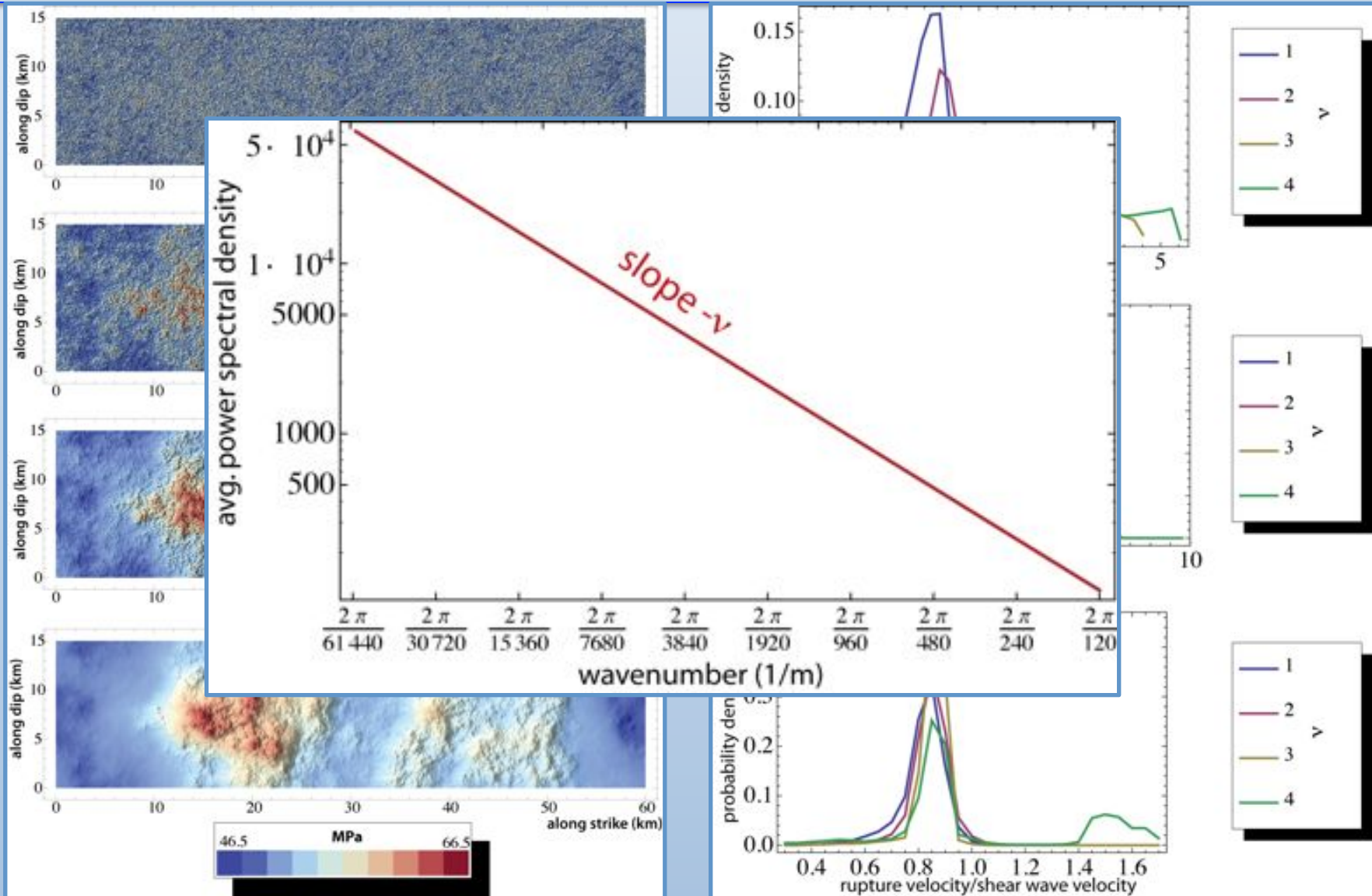
Influence of Autocorrelation: 2-Point Statistics

$v=1$

$v=2$

$v=3$

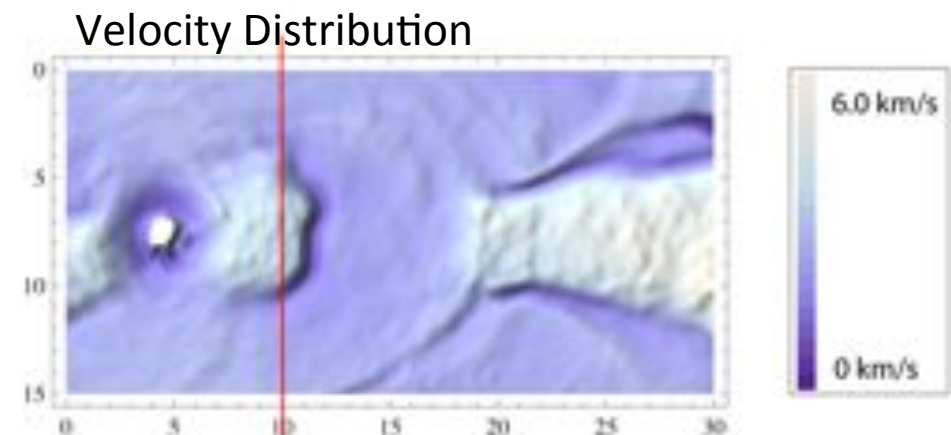
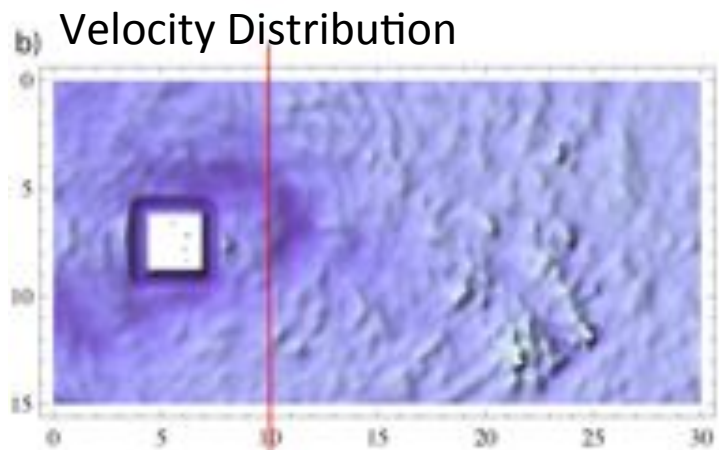
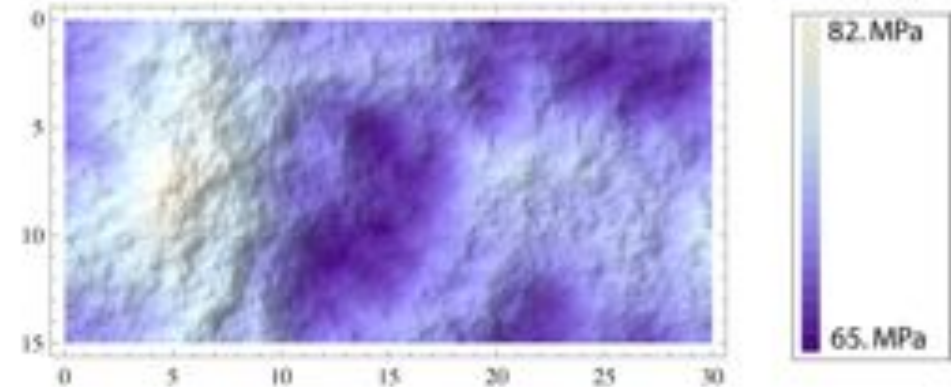
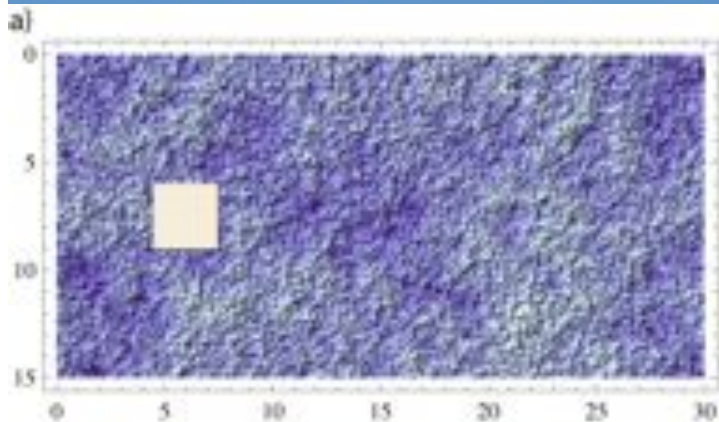
$v=4$



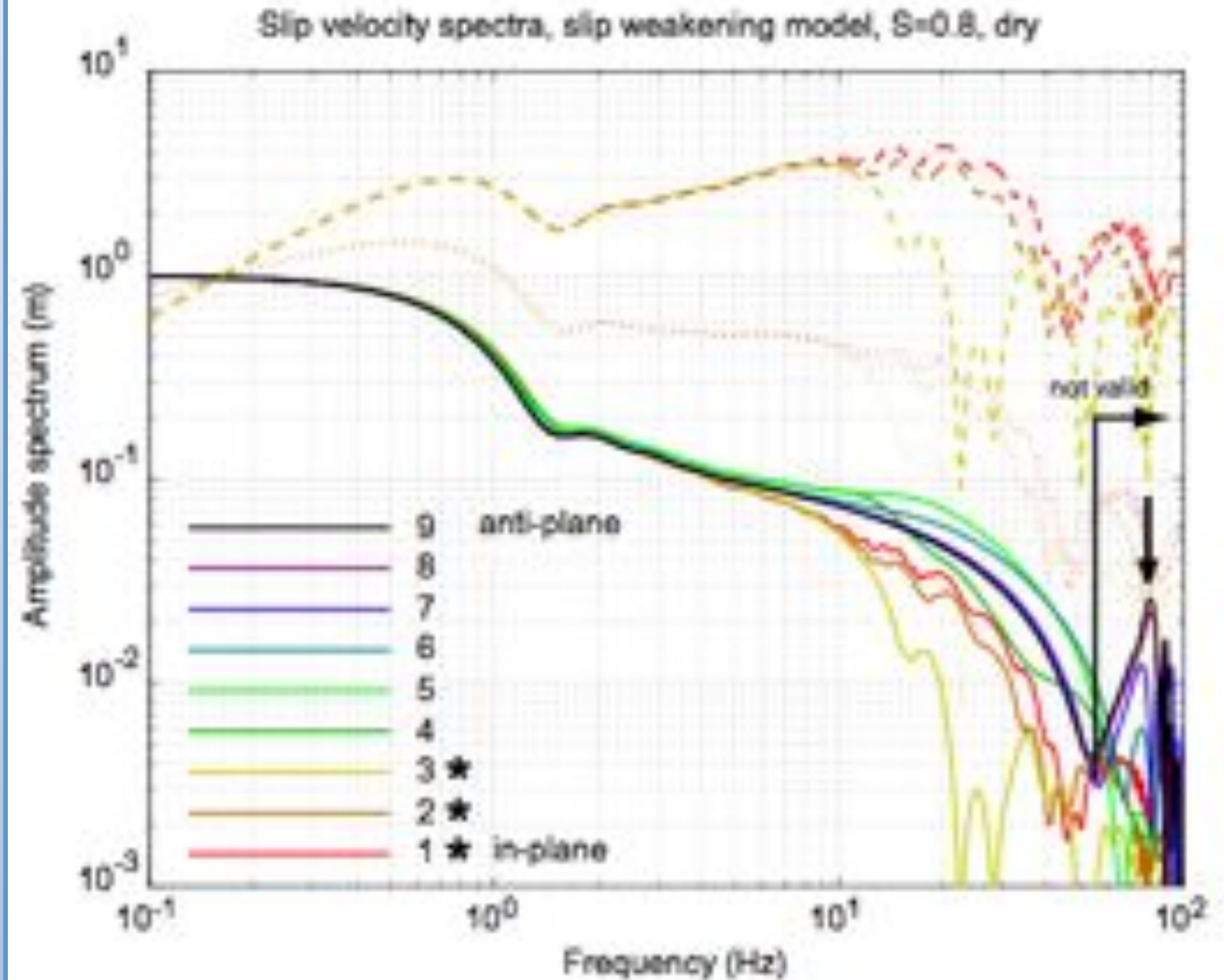
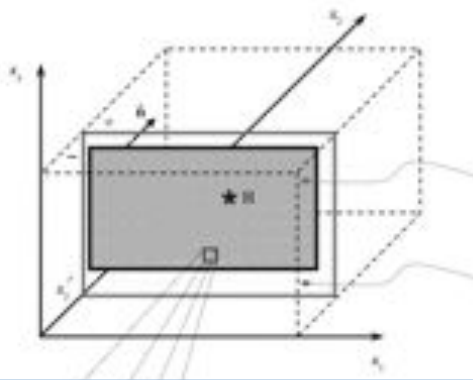
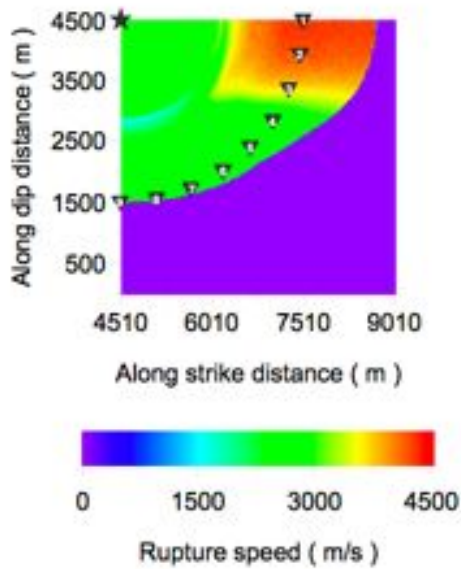
2-Point Statistics: Stress and Rupture Velocity on Fault

Stress Distribution: Power Spectrum K^{-2}

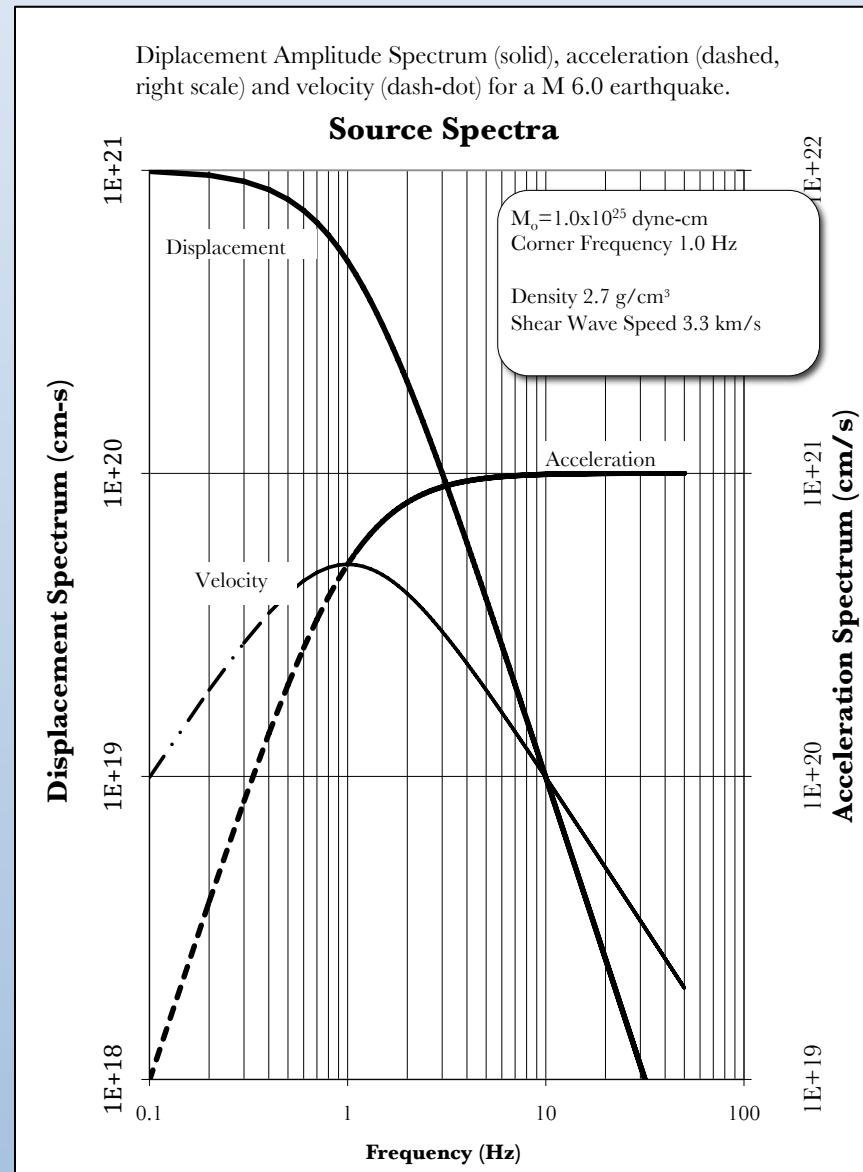
Stress Distribution: Power Spectrum K^{-4}



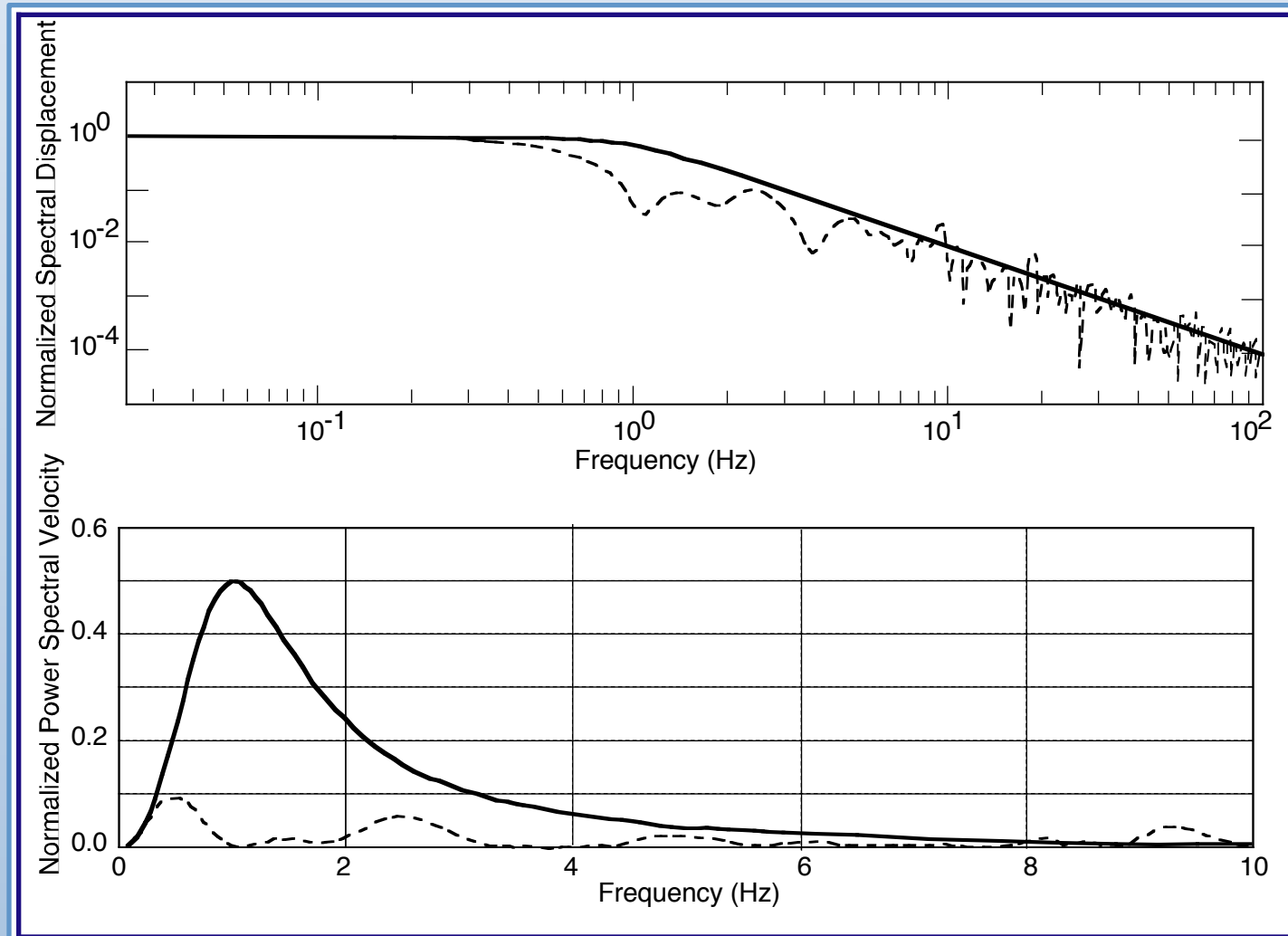
Spectra: Supershear & Subshear



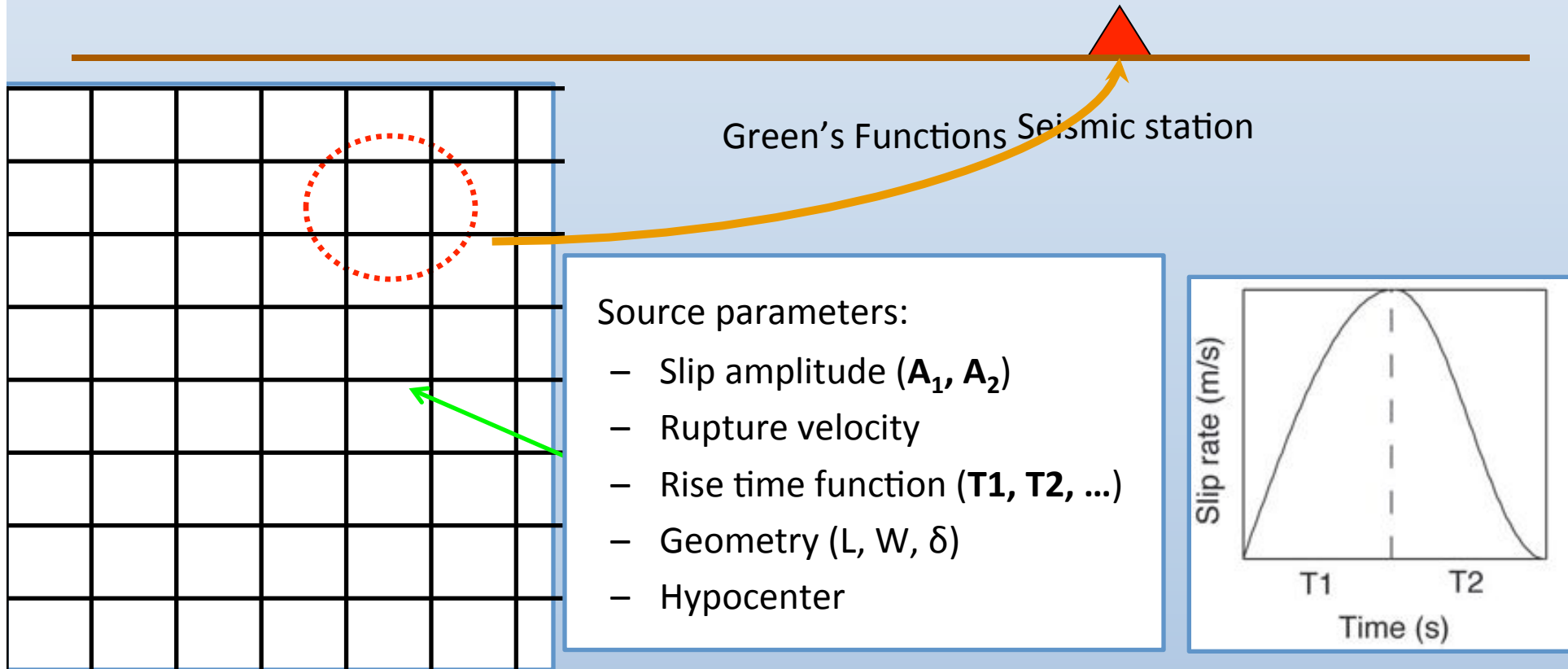
Source Spectrum



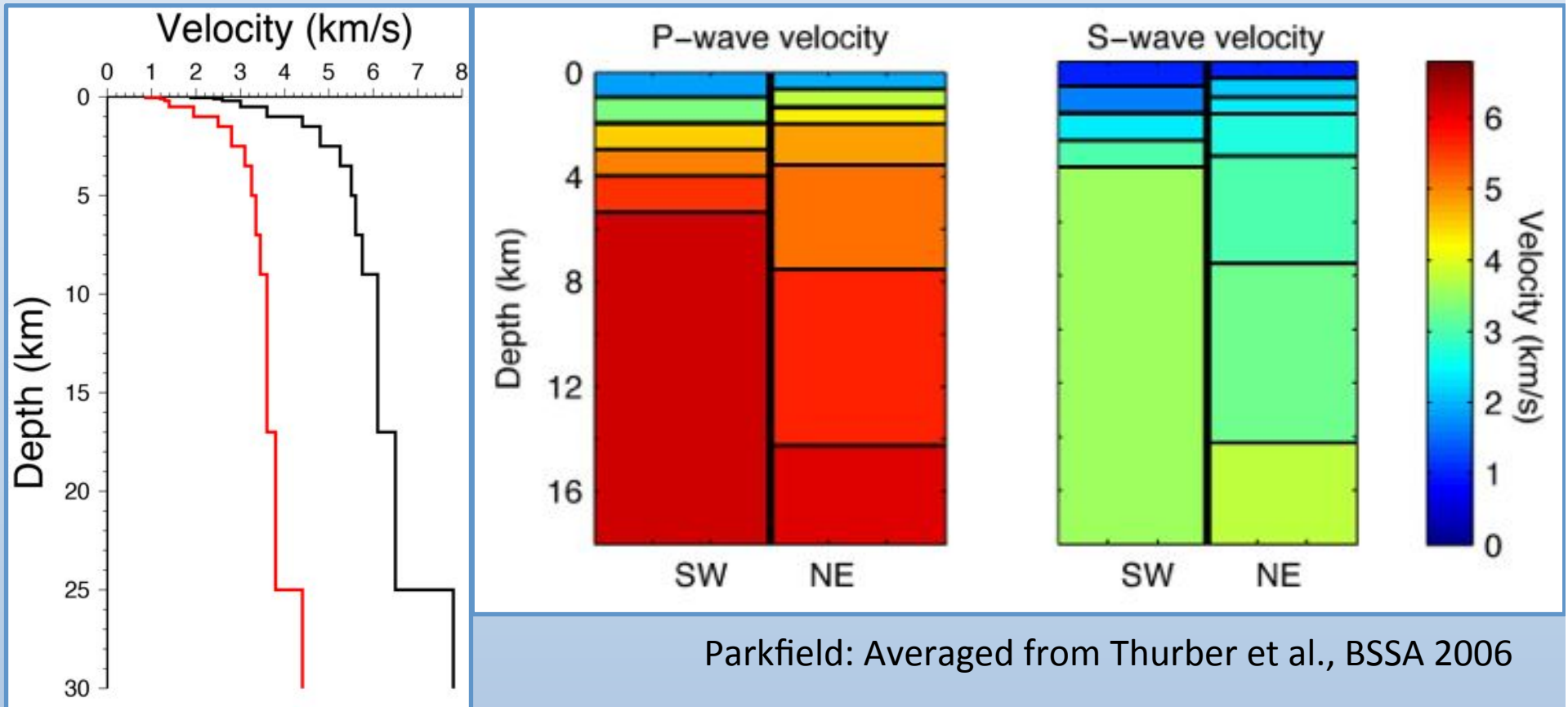
Energy Concentrated Near the Corner Frequency



Kinematics - forward modeling



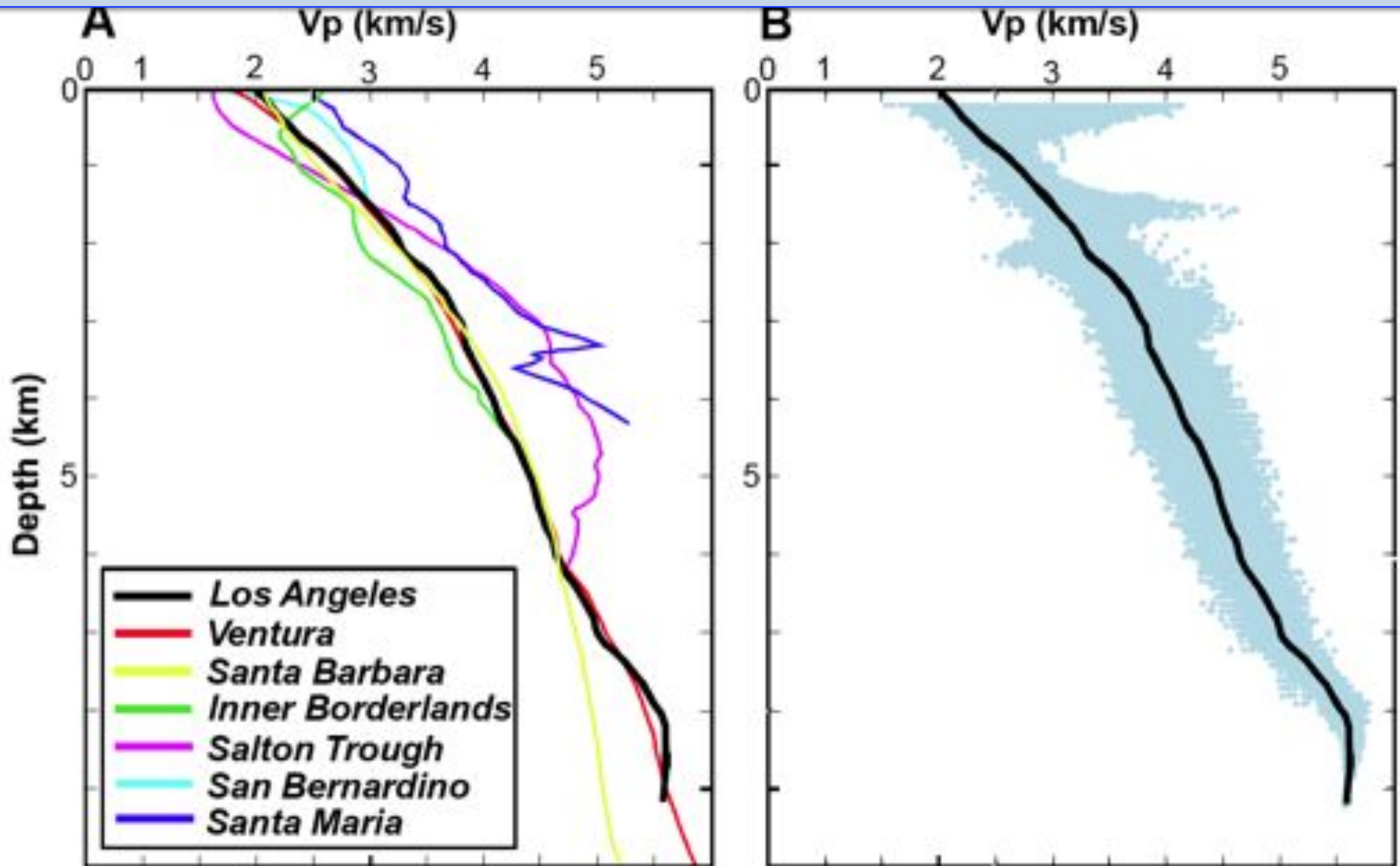
Velocity Structure



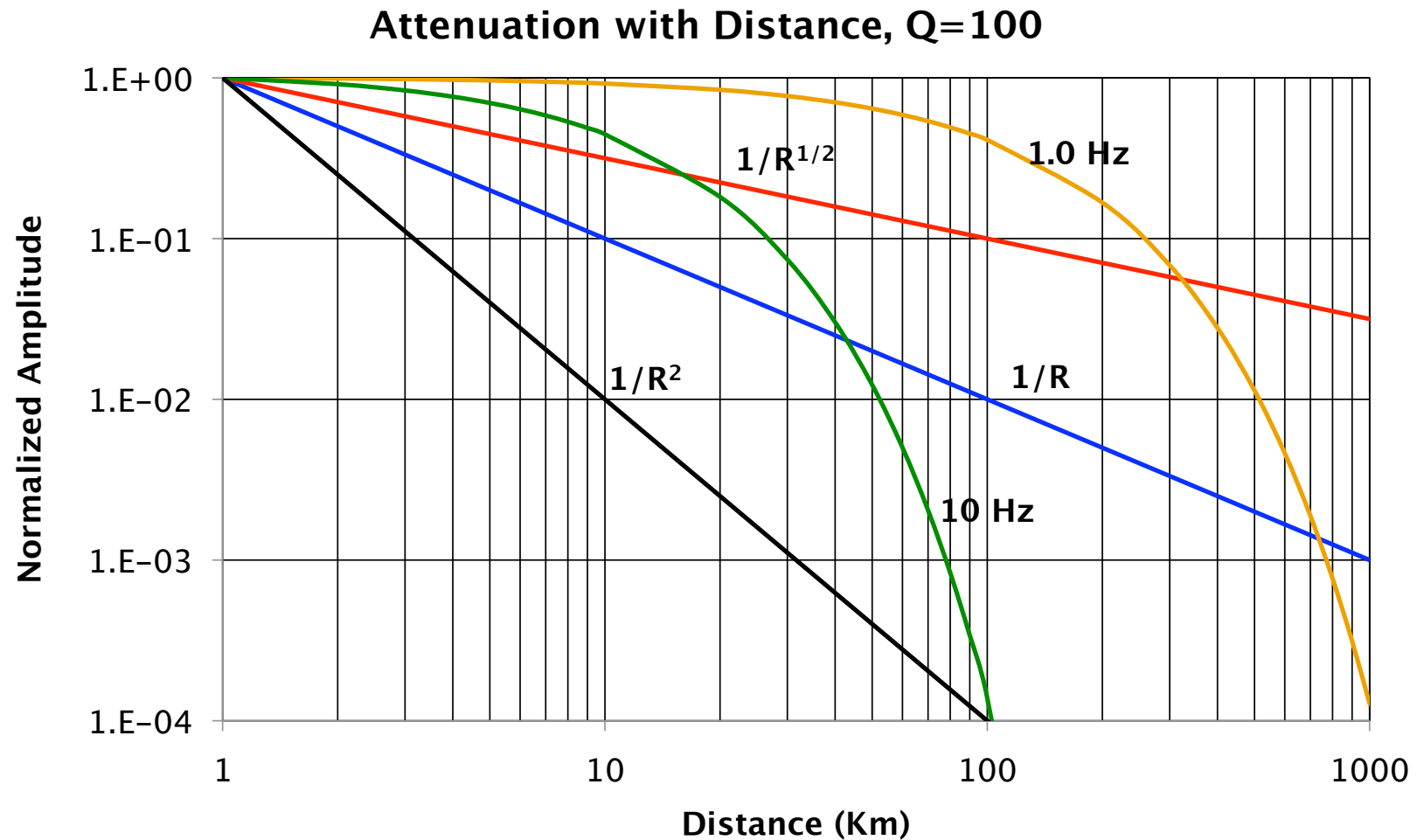
SCEC Validation

Parkfield: Averaged from Thurber et al., BSSA 2006

USR in SONGS Study Area



Amplitude Attenuation with Distance

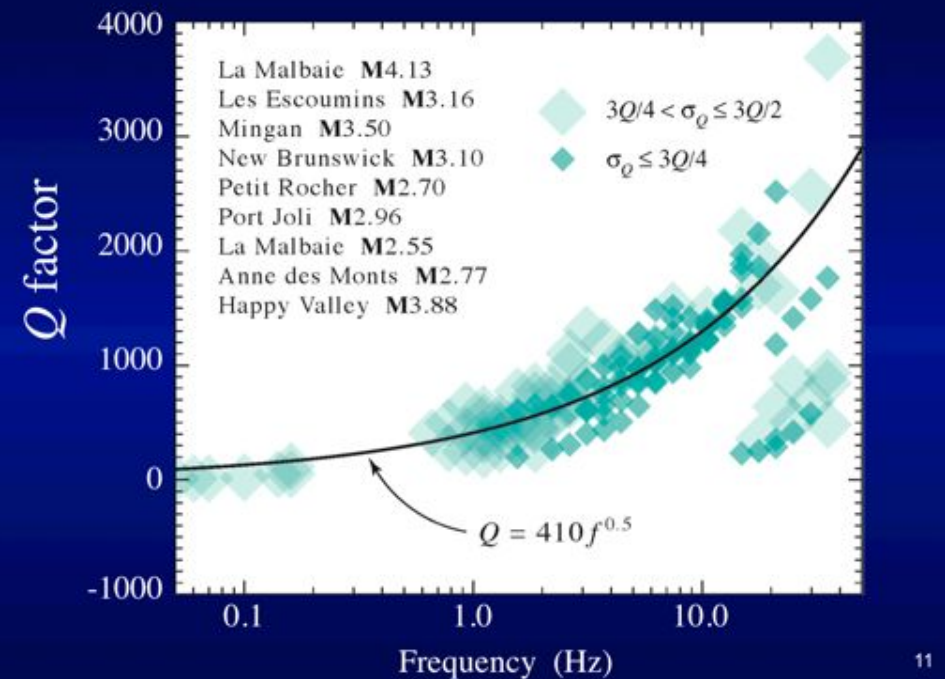
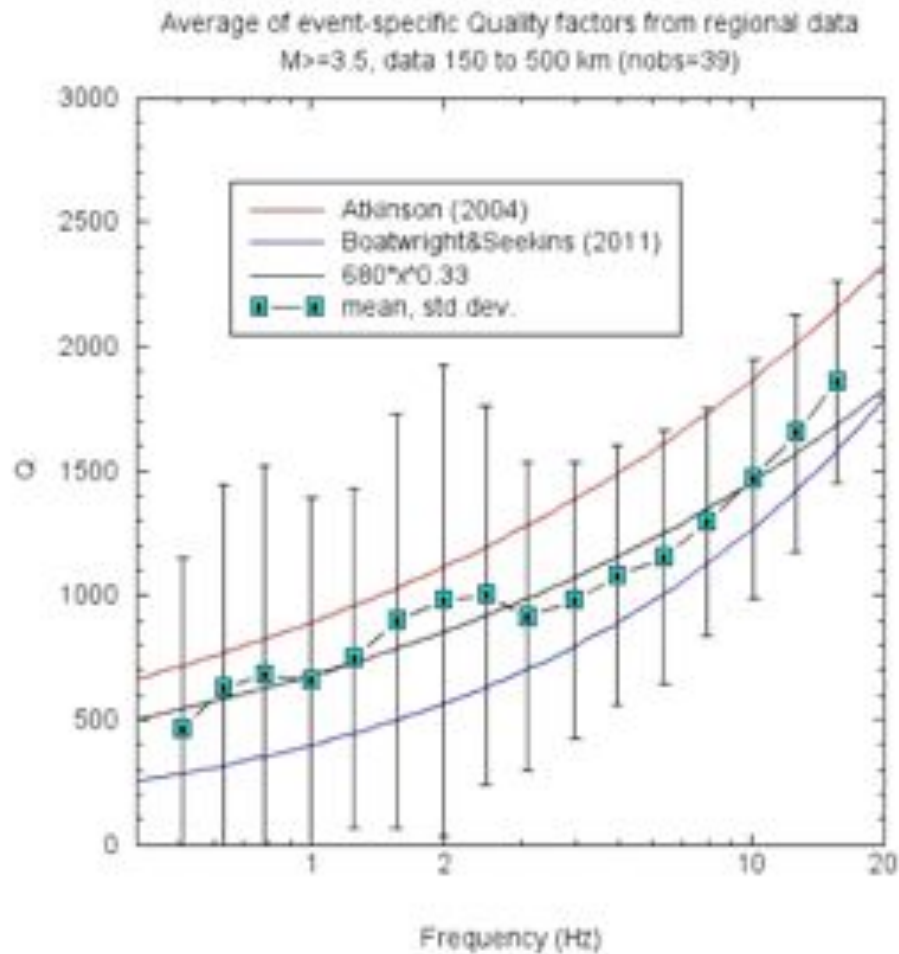


$$A(t) = A_0(1 - \pi / Q)^n \quad \text{for } t = 2n\pi / \omega$$

$$A(t) = A_0(1 - \omega t / 2Qn)^n$$

$$A(t) = A_0 e^{-\omega t / 2Q} \quad \text{for large } n, \text{ i.e., large time.}$$

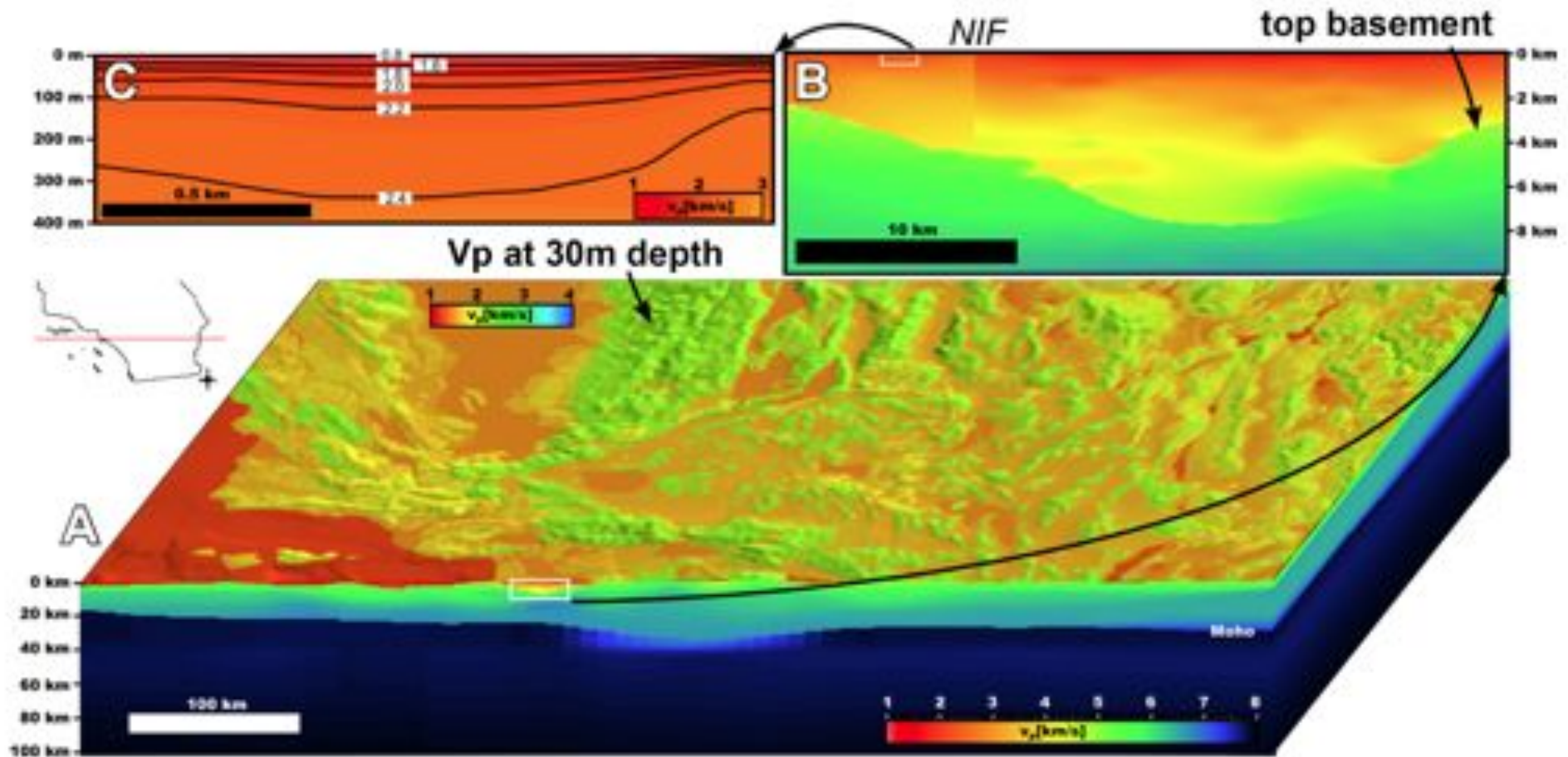
Attenuation



Boatwright and Seekins, 2012

11

Geotechnical Layer (GTL)



Shaw et al., (2013)

- GTL's are shallow (< 300 m) velocity descriptions that are necessary for many local seismological and engineering applications.
- The USR/CVM has an optional GTL overlay based on Vs30 measurements.

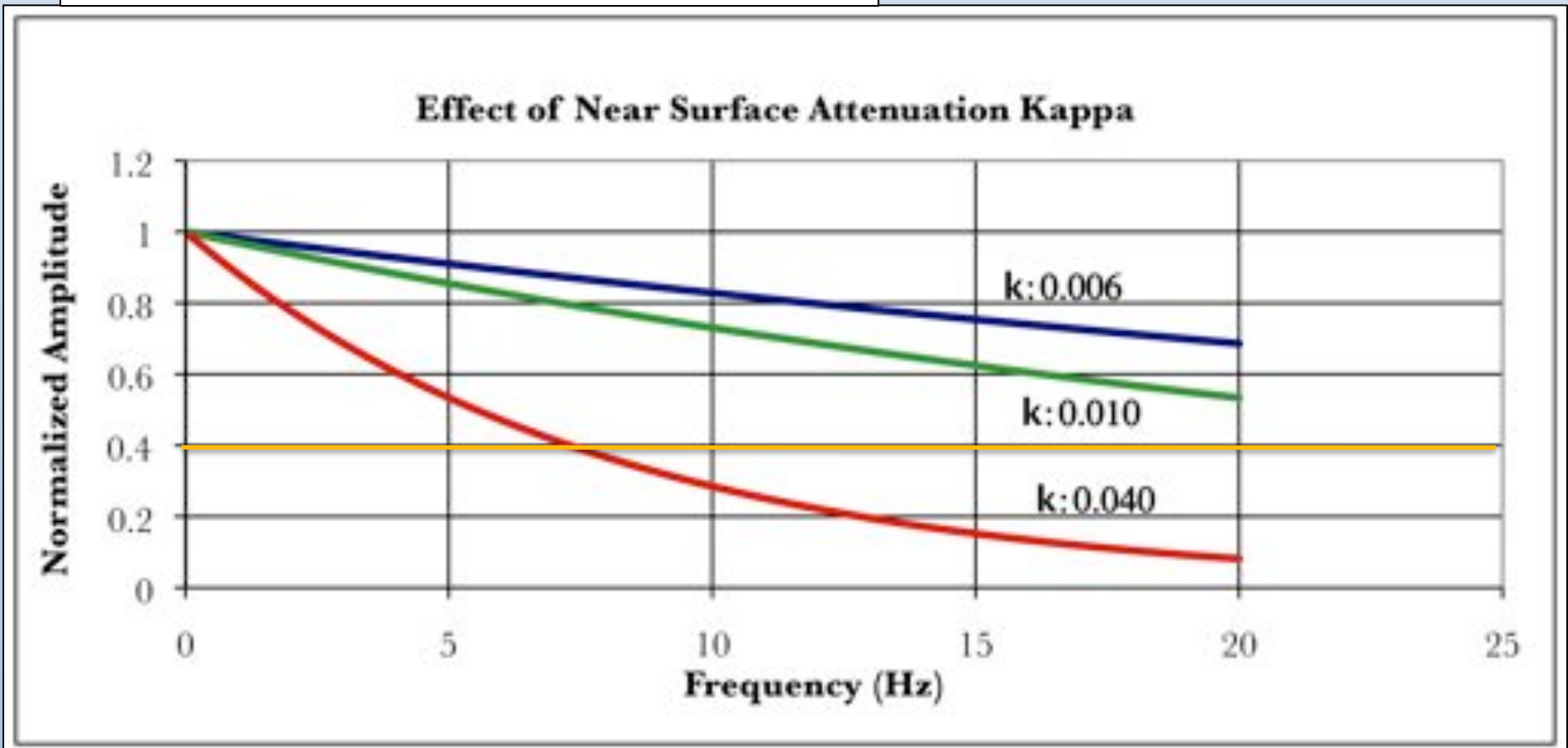
$$\kappa = \text{traveltime} / Q = \left(\frac{H}{V_s} \right) / Q$$

$$\text{Attenuation} = \exp(-\pi f \kappa)$$

$$\pi f \kappa = 1$$

$$f = 1 / \pi \kappa \rightarrow f_{\max}$$

Kappa and f_{\max}



Hartzell 1978

EARTHQUAKE AFTERSHOCKS AS GREEN'S FUNCTIONS

Stephen H. Hartzell

Institute of Geophysics and Planetary Physics
University of California, San Diego, La Jolla, California

Abstract. A method is presented for modeling earthquake strong ground motion, which uses the aftershocks associated with a large earthquake as Green's functions. A major earthquake, with a large rupture surface, is modeled by a collection of point sources distributed over the fault plane. The response of each point source is approximated by the ground motion of the closest associated aftershock. By using the aftershock responses, the effects of the true earth structure are included in the modeling process. This method is used to model the El Centro displacement record for the 1940 Imperial Valley earthquake.

Introduction

One technique often used to study the mechanics of earthquakes is to compute synthetic seismograms and compare them with data. There are two major problems which must be dealt with in the calculation of synthetic seismograms: 1) the description of the source, and 2) the calculation of the earth response. These are both difficult tasks, and one must invariably rely on approximations. Often the details of the focal mechanism are not known or poorly determined. Also, a realistic model of a moderate to large earthquake should take into consideration the finiteness of the source. One approximation which has proved useful is the superposition of point sources, phase delayed to account for rupture propagation. Summation of point sources has been used in media ranging from a full-space (Aki, 1968) to a layered half-space (Heaton and Haseberg, 1977).

The calculation of the earth response is typically done by assuming a model composed of homogeneous layers. With this simple model, standard methods can be applied, such as the reflectivity method (Fuchs and Müller, 1971) or the generalized ray method (Haseberg, 1968). However, situations continually arise where homogeneous layers are inappropriate, for example, a sedimentary basin thinning out against a mountain range. Recent studies by Egan and Haseberg (1977) and Chapman (1974, 1976) have relaxed some of the requirements in the generalized ray approach to allow uniformly dipping layers and model parameters which vary smoothly with depth. Also, work by Houston and Aki (1977), using an approximate method based on the discrete wave number representation of an elastic wave field, allows the calculation of synthetic seismograms in the presence of topography and irregular inter-

In this paper the earth response is empirically arrived at by the use of earthquake aftershock responses. Aftershocks are treated as approximate point dislocations. The ground motion associated with a given aftershock is then simply the Green's function for that aftershock's focal mechanism and position within the three-dimensional earth structure. With this approach, one need not know the actual focal mechanism. Also, the numerical and analytical difficulties of computing the earth response for an approximate earth model are avoided, and at the same time, the effects of the true earth structure are included.

Method

We require aftershock recordings from sources on the fault plane of the main event, whose ground motion we wish to model. These aftershocks should be well distributed over the fault plane and be of a sufficient number so that there are no "black" areas. The aftershocks should be well approximated as point sources. The ground motion due to the i -th aftershock, U_i , must be recorded at the same station that recorded the main event. We represent the fault plane of the main event by a distribution of point sources. The ground motion for the aftershock, U_i , which is closest to a given point source, is used as the point source response. The ground motion for the main event, U , is then approximated by the weighted and phase delayed summation over U_i :

$$U(t) = \sum_{i=1}^n [U_i(t) * Q_i(t)]H(t-t_i) \quad (1)$$

where

$$U_i(t) = S_i(t) * M_i(t) * R_i(t) \quad (2)$$

and * indicates convolution. The index i in Equations (1) and (2) runs over the n point sources on the fault plane. Q_i is a generalized scaling factor to be discussed below; H is the Heaviside unit step function; t_i is a phase delay term, which includes both the delay due to rupture propagation and the delay due to the travel time from the source to the receiver. S_i is the source function; M_i is the earth response; and R_i is the receiver function. The effects of S_i , M_i , and R_i are all included in the aftershock record U_i .

Irikura 1983

Semi-Empirical Estimation of Strong Ground Motions During Large Earthquakes

By KOJIRO IRIKURA

(Manuscript received March 22, 1983)

Abstract

A synthesis method is developed for estimating deterministically strong motions during the mainshock, using the records of small events such as foreshocks and aftershocks which occurred within the area of the mainshock fault. This synthesis formulation is based on the kinematic source model of Haskell type and the similarity law of earthquakes. The parameters for this synthesis are determined to be consistent with the scaling relations between the moments and the fault parameters such as fault length, width and dislocation rise time. If the ratio of the mainshock moment M_0 to the small event one M_0' is assumed to be N^3 , then the mainshock fault can be divided into $N \times N$ elements, each dimension of which is consistent with that of the small event and N events at each element may be superposed with a specific time delay to correct the difference in the rise time between the mainshock and the small event and to keep a constant slip velocity between them. By means of this method, the mainshock velocity motions are synthesized using the small event records obtained by velocity-type strong-motion seismographs for 1960 Izu-Hanto-Toho-Oki Earthquake ($M=6.3$). The resultant synthesized motions show a good agreement with the observed ones in the frequency range lower than 1 Hz. Further, the synthesis formulation is improved to be applicable to the higher frequency motions, especially acceleration motions. This revised synthesis for the higher frequency motions is effective when we use the records from the small event having the fault length $L_0 = V_r \tau$ (V_r : rupture velocity and τ : rise time of mainshock). The synthesized accelerograms by this revised method are in good agreement with the observed ones in the frequency range up to 5 Hz.

1. Introduction

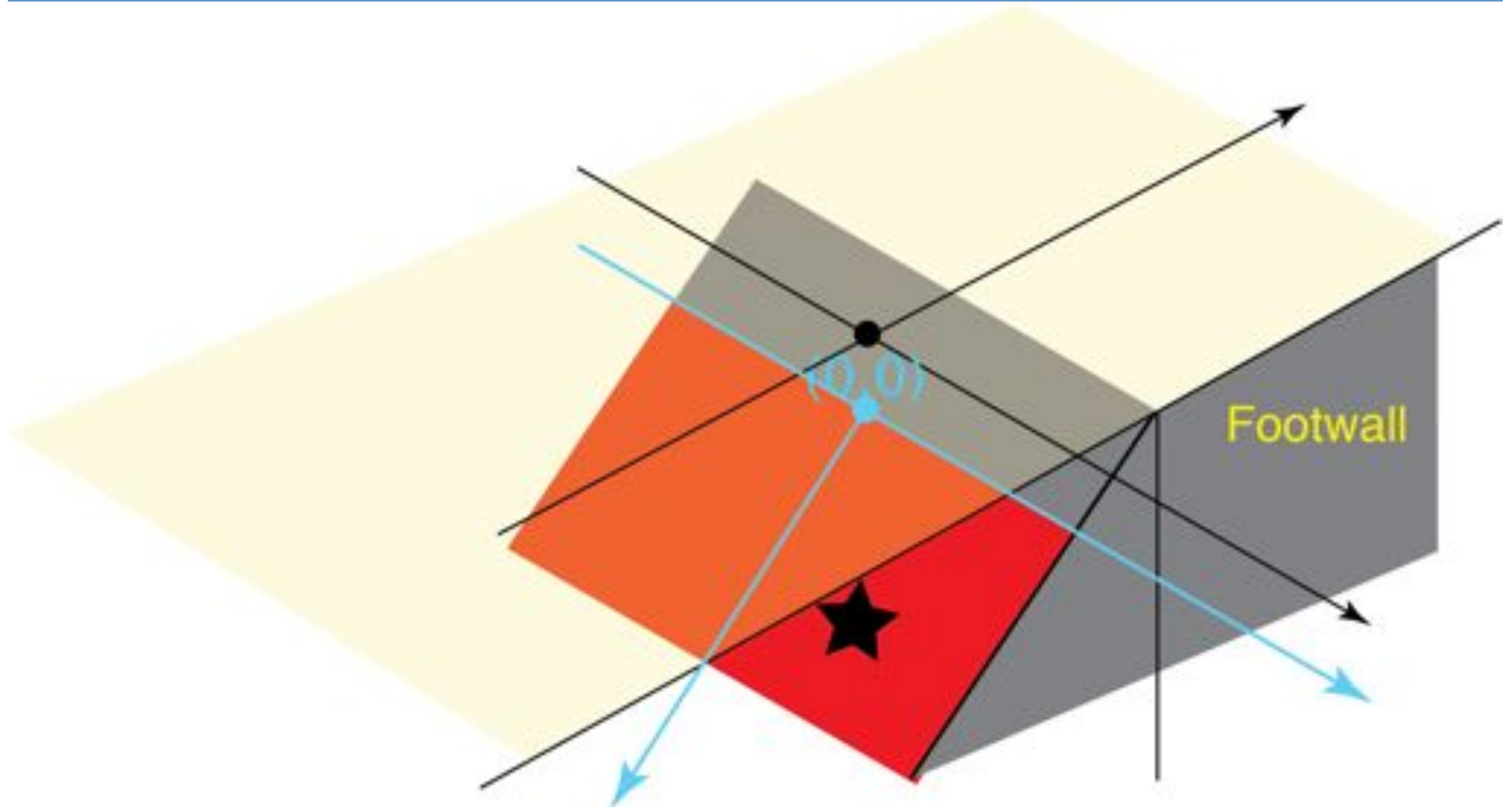
The investigation of the synthesis of strong ground motions in the near field has significantly lagged, compared with that of long period motions in the far field. This is caused by the difficulties of theoretical treatment for high frequency motions included in the strong motions. The investigators for earthquake engineering have been concerned with the strong motions from the need of engineering. Therefore, the input motions usually used for the evaluation of earthquake resistant design criteria have been synthesized for some time, independently of the physical considerations of the earthquake source. Recently, seismologists have begun to take an active interest in strong motions to study the details of faulting, as strong motion data have been accumulating in the near field. On the other hand, many investigators concentrate their attention of engineering interest on reliable estimates of the strong

SRC File

FAULT_WIDTH = 22.0
HYPO_ALONG_STK = 0.0
DLEN = 0.1
HYPO_DOWN_DIP = 14.75
DWID = 0.1
RAKE = 136
FAULT_LENGTH = 40.0
DEPTH_TO_TOP = 3.85
CORNER_FREQ = 0.15
MAGNITUDE = 6.94
LAT_TOP_CENTER = 37.0789
STRIKE = 128
LON_TOP_CENTER = -121.8410
DIP = 70
SEED = 9582093

FAULT_WIDTH (km)
FAULT_LENGTH (km)
DEPTH_TO_TOP (km)
LAT_TOP_CENTER (decimal degrees)
LON_TOP_CENTER (decimal degrees)
MAGNITUDE (Mw)
STRIKE (degrees)
DIP (degrees)
RAKE (decimal degrees)
HYPO_ALONG_STK (km)
HYPO_DOWN_DIP (km)
DWID (km)
DLEN (km)
CORNER_FREQ (Hz)
SEED (numerical seed value > 0)

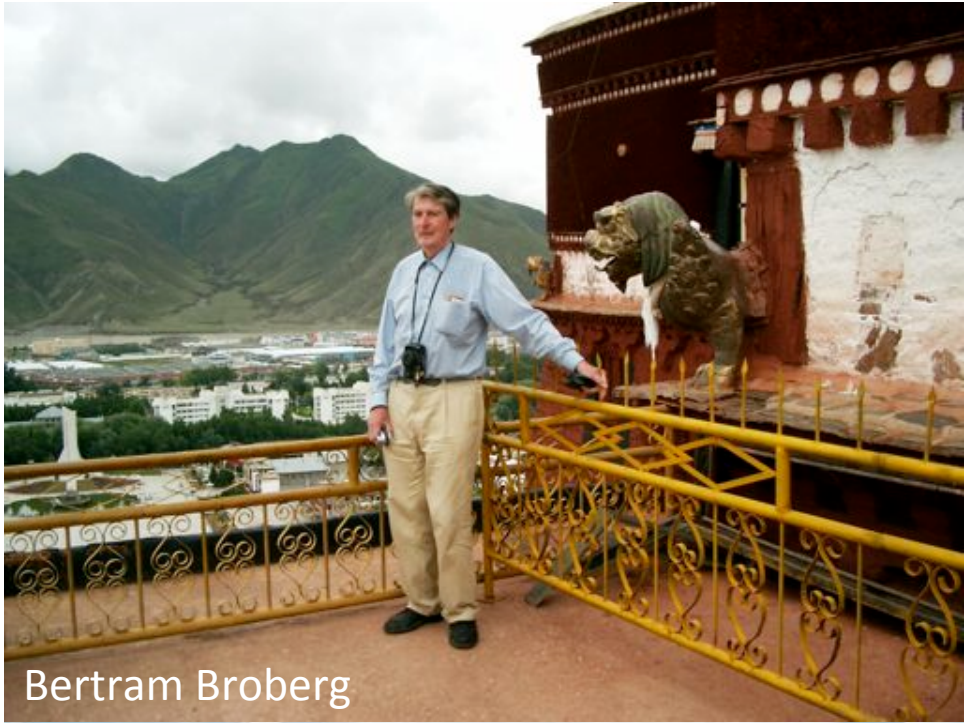
Origin: Geometry of Fault



Station List (.stl)

#BBP Station List for EQID=127 (Northridge)

#SLong	SLat	RSN	Rrup (km)	Vs30 (m/s)	HiPass (Hz)	LoPass (Hz)	Obs_File
-118.483	34.294	2005-LDM	5.9	629	0.1887	111.1111	NORTHR/2005-LDM_N.acc
-118.396	34.334	2006-PAC	7.0	2016	0.2105	111.1111	NORTHR/2006-PAC_N.acc
-118.710	34.232	2017-SSU	16.7	715	0.1263	111.1111	NORTHR/2017-SSU_N.acc
-118.380	34.114	2012-WON	20.3	1223	0.1927	111.1111	NORTHR/2012-WON_N.acc
-118.560	34.571	2016-H12	21.4	602	0.1502	111.1111	NORTHR/2016-H12_N.acc



Bertram Broberg



Teruo Maruyama



Ralph on the Kunlun Fault
VISES Sept. 28–Oct. 2, 2014



Questions?

Smiling Buddha

Thanks

